

# Entropy stable flux correction for hydrostatic reconstruction scheme for shallow water flows

Sergii Kivva\*

## Abstract

First-order hydrostatic reconstruction (HR) schemes for shallow water equations are highly diffusive whereas high-order schemes can produce entropy-violating solutions. Our goal is to develop a flux correction with maximum antidiffusive fluxes to obtain entropy solutions of shallow water equations with variable bottom topography. For this purpose, we consider a hybrid explicit HR scheme whose flux is a convex combination of first-order Rusanov flux and high-order flux. The conditions under which the explicit first-order HR scheme for shallow water equations satisfies the fully discrete entropy inequality have been studied. The flux limiters for the hybrid scheme are calculated from a corresponding optimization problem. Constraints for the optimization problem consist of inequalities that are valid for the first-order HR scheme and applied to the hybrid scheme. We apply the discrete cell entropy inequality with the proper numerical entropy flux to single out a physically relevant solution to the shallow water equations. A nontrivial approximate solution of the optimization problem yields expressions to compute the required flux limiters. Numerical results of testing various HR schemes on different benchmarks are presented.

**Keywords**— fully discrete entropy inequality, flux corrected transport, shallow water equations, hydrostatic reconstruction scheme, linear programming

**Mathematics Subject Classification (2010)** MSC 65M08 · MSC 65M22 · 76M12

## 1 Introduction

In this paper, we consider a design of entropy stable flux correction for a hydrostatic reconstruction scheme for shallow water equations with variable bottom topography. For simplicity, without loss of generality, we focus on the Saint-Venant system of one-dimensional shallow water equations, given by

$$\begin{aligned}\partial_t h + \partial_x Q &= 0, \\ \partial_t Q + \partial_x \left( \frac{Q^2}{h} + g \frac{h^2}{2} \right) &= -gh \partial_x z,\end{aligned}\tag{1.1}$$

subject to the initial conditions

$$h(x, 0) = h_0(x), \quad Q(x, 0) = Q_0(x),\tag{1.2}$$

---

\*Institute of Mathematical Machines and System Problems, National Academy of Sciences, Ukraine

where  $h(x, t)$  is the water depth,  $Q(x, t)$  is the water discharge,  $g$  is the gravitational constant, and  $z(x)$  is the bottom topography. The system (1.1) is considered in a certain spatial domain  $D$ , and if  $D \neq R$ , then on the boundary of  $D$  a corresponding boundary conditions should be specified.

In vector form, the system (1.1) can be written as

$$\frac{\partial \mathbf{u}}{\partial t} + \frac{\partial}{\partial x} \mathbf{f}(\mathbf{u}) = \mathbf{s}, \quad (1.3)$$

where  $\mathbf{u} = (h, Q)^T$  is the vector of conserved variables,  $\mathbf{f} = (Q, Q^2/h + gh^2/2)^T$  is the flux vector, and  $\mathbf{s} = (0, ghz_x)^T$  is the source vector.

It is well known [19] that solutions of (1.1)-(1.2) may develop singularities in finite time even for a smooth initial condition. Hence, we should interpret (1.1) in the sense of distribution and search for weak solutions. However, such weak solutions are not unique. To single out a unique physically relevant weak solution, the latter should satisfy

$$\frac{\partial U(\mathbf{u})}{\partial t} + \frac{\partial F(\mathbf{u})}{\partial x} \leq 0 \quad (1.4)$$

in the sense of distribution for every entropy pair  $(U, F)$ . Here  $U$  is a convex function of  $\mathbf{u}$ , the so-called entropy function, and  $F$  is its entropy flux that satisfies

$$F_{\mathbf{u}}^T(\mathbf{u}) = U_{\mathbf{u}}(\mathbf{u}) \mathbf{f}_{\mathbf{u}}(\mathbf{u}). \quad (1.5)$$

For shallow water equations (1.1) with bottom topography  $z(x)$ , the total energy

$$U(\mathbf{u}) = \frac{1}{2} \left( \frac{Q^2}{h} + gh^2 \right) + ghz, \quad (1.6)$$

serves as an entropy function with entropy flux

$$F(\mathbf{u}) = \frac{Q^3}{2h^2} + ghQ + gQz. \quad (1.7)$$

We discretize (1.3) by the difference scheme

$$\frac{1}{\Delta t} (\hat{\mathbf{v}}_i - \mathbf{v}_i) + \frac{1}{\Delta x} [\mathbf{g}_{i+1/2} - \mathbf{g}_{i-1/2}] = \mathbf{s}_i, \quad (1.8)$$

where the numerical flux  $\mathbf{g}_{i+1/2}$  is calculated as

$$\mathbf{g}_{i+1/2} = \mathbf{g}_{i+1/2}^L + \alpha_{i+1/2} [\mathbf{g}_{i+1/2}^H - \mathbf{g}_{i+1/2}^L]. \quad (1.9)$$

Here,  $\mathbf{v}_i = \mathbf{v}(x_i, t) = (y(x_i, t), q(x_i, t))^T$  is the discrete solution at the grid point  $(x_i = i\Delta x, t)$ ;  $\hat{\mathbf{v}}_i = \mathbf{v}(x_i, t + \Delta t)$ ;  $\Delta x$  and  $\Delta t$  are the spatial and temporal computational grid size, respectively.  $\mathbf{g}_{i+1/2}^H$  and  $\mathbf{g}_{i+1/2}^L$  are a high-order and low-order numerical fluxes such that  $\mathbf{g}_{i+1/2} = \mathbf{g}(\mathbf{v}_{i-l+1}, \dots, \mathbf{v}_{i+r})$  is the Lipschitz continuous numerical flux consistent with the differential flux, that is  $\mathbf{g}(\mathbf{u}, \dots, \mathbf{u}) = \mathbf{f}(\mathbf{u})$  for all flux-limiters  $\alpha_{i+1/2} \in [0, 1]$ .

The expression in square brackets on the right-hand side of (1.5) can be considered as an antidiffusive flux. For flux-correction we compute the flux limiters  $\alpha_{i+1/2}$  as an approximate solution to the corresponding optimization problem. The classical two-step Flux-Corrected

Transport (FCT) was firstly developed by Oran and Boris [4] to solve the transient continuity equation. The procedure of two-step flux correction consists of computing the time-advanced low-order solution in the first step and correcting the solution by adding antidiffusive fluxes in the second step to produce accurate and monotone results. The antidiffusive fluxes, which define as the difference between the high and low-order fluxes, are limited in such a way that neither new extrema are created nor existing extrema are increased. Later, Zalesak [31, 32] extended FCT to multidimensional explicit difference schemes. In [32], using characteristic variables, Zalesak proposed FCT algorithms for nonlinear systems of conservation laws. Several implicit FEM-FCT schemes for unstructured grids were proposed by Kuzmin and coworkers [17, 18]. However, the known FCT algorithms do not guarantee entropy solutions for hyperbolic conservation laws.

We discretize the entropy inequality (1.4) as follows

$$U(\hat{\mathbf{v}}_i) - U(\mathbf{v}_i) + \frac{\Delta t}{\Delta x} [G_{i+1/2} - G_{i-1/2}] \leq 0 \quad (1.10)$$

where  $G_{i+1/2} = G(\mathbf{v}_{i-l+1}, \dots, \mathbf{v}_{i+r})$  is the numerical entropy flux consistent with the differential one  $G(\mathbf{u}, \dots, \mathbf{u}) = F(\mathbf{u})$ .

A difference scheme (1.8) is called *entropy stable* if computed solutions satisfy the discrete cell entropy inequality (1.6). We mention here the pioneering studies of entropy stable schemes by Lax [19]. Entropy stable schemes were developed by several authors [7, 10, 12, 13, 20, 25, 29, 30]. To single out a physically relevant solution, we use the so-called proper numerical entropy flux, the concept of which was formulated by Merriam [21] and Sonar [27]. Zhao and Wu [33] proved that three-point monotone semi-discrete schemes in conservative form satisfy the corresponding semi-discrete entropy inequality with the proper numerical entropy flux. Fully discrete entropy stable schemes with the proper numerical entropy flux for scalar conservation laws were obtained in [15, 16]. The numerical entropy flux  $G(\mathbf{v}_{i-l+1}, \dots, \mathbf{v}_{i+r})$  for  $F$  is not unique. The distinguishing feature of the proper numerical entropy flux among others is that it satisfies property (1.5) of the differential entropy flux.

In this paper, we apply a first-order hydrostatic reconstruction (HR) scheme as a low-order scheme to design flux correction. A first-order HR scheme was originally developed by Audusse et al. [1], and it does not properly account for the acceleration due to a sloped bottom [8] for shallow downhill flow. Morales de Luna et al. [23] improved the original first-order HR scheme for partially wet interfaces. Using a technique of subcell reconstructions, Chen and Noelle [6] proposed a new reconstruction with a better approximation of the source term for shallow downhill flows. The main properties of the original HR scheme or its modifications are positivity preserving, well-balanced, and satisfying a semi-discrete in-cell entropy inequality. Unfortunately, it is well known that semi-discrete entropy inequalities are insufficient to obtain a suitable convergence to the entropy weak solution or to get relevant energy estimates. Audusse et al. [2] showed that the HR scheme combined with a kinetic solver satisfies a fully discrete entropy inequality with an error term coming from the topography. Thus, we can expect the convergence of this scheme for Lipschitz continuous bathymetry. Berthon et al. [3] suggested to introduce artificial viscosity into the HR scheme to get fully discrete entropy inequalities.

Using the approach proposed in [15, 16], we construct a flux correction for 1D shallow water equations (1.1) to obtain numerical entropy solutions for which the antidiffusive fluxes are maximal. For this, the flux limiters for the hybrid scheme (1.8)-(1.9) are computed from the optimization problem with constraints that are valid for the low-order scheme. An approximate solution to the optimization problem yields the desired flux correction formulas. Moreover, con-

sidering the flux limiters as functions of the numerical solution, we prove the unique solvability of the hybrid scheme (1.8)-(1.9) under general assumptions on them. We show that the approximate limiters satisfy the assumptions under which the hybrid scheme has a unique solution. The developed approach is a novel view on the known FCT method.

The paper is organized as follows. In Section 2, we present estimates that are valid for an explicit first-order HR scheme with the Rusanov numerical flux. Section 3 defines the proper numerical entropy flux and studies the conditions under which the explicit HR scheme for homogeneous and inhomogeneous shallow water equations satisfies the fully discrete entropy inequality. The unique solvability of flux correction for the HR scheme, the optimization problem for finding flux limiters, and the algorithm for its solution are described in Section 4. An approximate solution of the optimization problem is derived in Section 5. The results of numerical experiments with different HR schemes are given in Section 6. Concluding remarks are drawn in Section 7.

## 2 First-Order Hydrostatic Reconstruction Scheme

We consider an explicit first-order HR scheme of Chen and Noelle [6] in the form

$$\hat{\mathbf{v}}_i - \mathbf{v}_i + \frac{\Delta t}{\Delta x} \left[ \mathbf{g}_{i+1/2}^L(\mathbf{v}_{i+1/2}^-, \mathbf{v}_{i+1/2}^+) - \mathbf{g}_{i-1/2}^L(\mathbf{v}_{i-1/2}^-, \mathbf{v}_{i+1/2}^+) \right] = \Delta t \mathbf{s}_i, \quad (2.1)$$

where  $\mathbf{g}_{i+1/2}^L$  is the Rusanov numerical flux [26] consistent with the differential flux  $\mathbf{f}$  and given by

$$\mathbf{g}_{i+1/2}^L(\mathbf{v}_{i+1/2}^-, \mathbf{v}_{i+1/2}^+) = \frac{1}{2} \left( \mathbf{f}(\mathbf{v}_{i+1/2}^-) + \mathbf{f}(\mathbf{v}_{i+1/2}^+) - c_{i+1/2}(\mathbf{v}_{i+1/2}^+ - \mathbf{v}_{i+1/2}^-) \right). \quad (2.2)$$

The vectors of conservative variables  $\mathbf{v}_{i+1/2}^\pm$  are given by

$$\mathbf{v}_{i+1/2}^- = \begin{pmatrix} y_{i+1/2}^- \\ y_{i+1/2}^- u_i \end{pmatrix}, \quad \mathbf{v}_{i+1/2}^+ = \begin{pmatrix} y_{i+1/2}^+ \\ y_{i+1/2}^+ u_{i+1} \end{pmatrix}, \quad u_i = \frac{\sqrt{2} y_i q_i}{\sqrt{y_i^4 + \max(y_i^4, \epsilon)}}, \quad (2.3)$$

where  $\epsilon$  is a small a-priori chosen positive number. The water depths are calculated as

$$y_{i+1/2}^- = \min(w_i - z_{i+1/2}, y_i), \quad y_{i+1/2}^+ = \min(w_{i+1} - z_{i+1/2}, y_{i+1}) \quad (2.4)$$

with water levels  $w_i = z_i + y_i$ , and the cell interface bottom

$$z_{i+1/2} = \min(\max(z_i, z_{i+1}), \min(w_i, w_{i+1})). \quad (2.5)$$

The source term  $\mathbf{s}_i = -\mathbf{s}_{i-1/2}^+ + \mathbf{s}_{i+1/2}^- = (0, -s_{i-1/2}^+)^T + (0, s_{i+1/2}^-)^T$  is discretized as

$$\begin{aligned} s_{i+1/2}^- &= -g \frac{y_i + y_{i+1/2}^-}{2} \frac{z_i - z_{i+1/2}}{\Delta x}, \\ s_{i+1/2}^+ &= -g \frac{y_{i+1/2}^+ + y_{i+1}}{2} \frac{z_{i+1} - z_{i+1/2}}{\Delta x}. \end{aligned} \quad (2.6)$$

Finally, the local speed  $c_{i+1/2}$  in (2.2) is calculated using the eigenvalues of the Jacobian  $\mathbf{f}_u(\mathbf{u})$  as follows

$$c_{i+1/2} = \max \left( |u_i| + \sqrt{g y_{i+1/2}^-}, |u_{i+1}| + \sqrt{g y_{i+1/2}^+} \right). \quad (2.7)$$

The following theorem gives estimates for the numerical solution of the HR scheme (2.1).

**Theorem 2.1.** Assume that  $c_{i+1/2} \geq \max(|u_i|, |u_{i+1}|)$  for all  $i$ . Then for

$$\Delta t \leq \frac{2\Delta x}{\max_i (c_{i+1/2} - u_{i+1} + c_{i-1/2} + u_{i-1})}, \quad (2.8)$$

the following inequalities hold for the numerical solution of the system of equations (2.1)-(2.2)

$$\begin{aligned} \frac{\Delta x}{\Delta t} \min(w_i, w_{i-1/2}^-, w_{i+1/2}^+) &\leq \frac{\Delta x}{\Delta t} \hat{w}_i - \frac{u_i + u_{i+1}}{2} z_{i+1/2} - \left( \frac{c_{i+1/2} - u_{i+1}}{2} w_i - \frac{c_{i+1/2} + u_i}{2} w_{i+1/2}^- \right) \\ &+ \frac{u_i + u_{i-1}}{2} z_{i-1/2} - \left( \frac{c_{i-1/2} + u_{i-1}}{2} w_i - \frac{c_{i-1/2} - u_i}{2} w_{i-1/2}^+ \right) \leq \frac{\Delta x}{\Delta t} \max(w_i, w_{i-1/2}^-, w_{i+1/2}^+), \end{aligned} \quad (2.9)$$

$$\begin{aligned} \frac{\Delta x}{\Delta t} \min(q_i, q_{i-1/2}^-, q_{i+1/2}^+) &\leq \frac{\Delta x}{\Delta t} \hat{q}_i - \left( \frac{c_{i+1/2} - u_{i+1}}{2} q_i - \frac{c_{i+1/2} + u_i}{2} q_{i+1/2}^- \right) \\ &+ \frac{g}{2} \left[ \frac{1}{2} (y_{i+1/2}^{-2} + y_{i+1/2}^{+2}) + (y_i + y_{i+1/2}^-)(z_{i+1/2} - z_i) \right] \\ &- \frac{g}{2} \left[ \frac{1}{2} (y_{i-1/2}^{-2} + y_{i-1/2}^{+2}) + (y_i + y_{i-1/2}^+)(z_{i-1/2} - z_i) \right] \\ &- \left( \frac{c_{i-1/2} + u_{i-1}}{2} q_i - \frac{c_{i-1/2} - u_i}{2} q_{i-1/2}^+ \right) \leq \frac{\Delta x}{\Delta t} \max(q_i, q_{i-1/2}^-, q_{i+1/2}^+), \end{aligned} \quad (2.10)$$

where  $w_{i+1/2}^\pm = y_{i+1/2}^\pm + z_{i+1/2}$ .

*Proof.* Let us prove inequalities (2.9). Inequalities (2.10) are proved similarly.

We rewrite the equation (2.1) for the conservative variable  $y_i$  in the form

$$\begin{aligned} \frac{\Delta x}{\Delta t} \hat{y}_i &= \frac{\Delta x}{\Delta t} y_i - \frac{c_{i+1/2} + u_i}{2} y_{i+1/2}^- - \frac{c_{i-1/2} - u_i}{2} y_{i-1/2}^+ \\ &+ \frac{c_{i+1/2} - u_{i+1}}{2} y_{i+1/2}^+ + \frac{c_{i-1/2} + u_{i-1}}{2} y_{i-1/2}^-. \end{aligned} \quad (2.11)$$

Substituting the water level  $w_i$  in (2.11) instead of the water depth  $y_i$ , we obtain

$$\begin{aligned} \frac{\Delta x}{\Delta t} \hat{w}_i &= \left( \frac{\Delta x}{\Delta t} - \frac{c_{i+1/2} - u_{i+1}}{2} - \frac{c_{i-1/2} + u_{i-1}}{2} \right) w_i + \frac{c_{i+1/2} - u_{i+1}}{2} w_{i+1/2}^+ \\ &+ \frac{c_{i-1/2} + u_{i-1}}{2} w_{i-1/2}^- + \frac{u_i + u_{i+1}}{2} z_{i+1/2} - \frac{u_i + u_{i-1}}{2} z_{i-1/2} \\ &+ \left( \frac{c_{i+1/2} - u_{i+1}}{2} w_i - \frac{c_{i+1/2} + u_i}{2} w_{i+1/2}^- \right) + \left( \frac{c_{i-1/2} + u_{i-1}}{2} w_i - \frac{c_{i-1/2} - u_i}{2} w_{i-1/2}^+ \right). \end{aligned} \quad (2.12)$$

Note that under the condition (2.8), the first three terms in the right-hand side of (2.12) are a convex combination of  $w_i, w_{i+1/2}^+$ , and  $w_{i-1/2}^-$ , which proves the theorem.  $\square$

**Remark 2.1.** We note that if  $c_{i+1/2}$  satisfies the following inequalities

$$\begin{aligned} \frac{\Delta x}{\Delta t} y_i - \frac{c_{i+1/2} + u_i}{2} y_{i+1/2}^- - \frac{c_{i-1/2} - u_i}{2} y_{i-1/2}^+ &\geq 0, \\ c_{i+1/2} - u_{i+1} &\geq 0, \quad c_{i-1/2} + u_{i-1} \geq 0, \end{aligned} \quad (2.13)$$

then the difference scheme (2.11) preserves the non-negativity of the water depth  $y$ .

### 3 Cell Entropy Inequality for Fully Discrete HR Scheme

In this section we study the cell entropy inequality for the fully discrete HR scheme (2.1)-(2.2).

We consider a homogeneous three-point low-order scheme in the form

$$\hat{\mathbf{v}}_i - \mathbf{v}_i + \frac{\Delta t}{\Delta x} [\mathbf{g}_{i+1/2}^L(\mathbf{v}_i, \mathbf{v}_{i+1}) - \mathbf{g}_{i-1/2}^L(\mathbf{v}_{i-1}, \mathbf{v}_i)] = 0, \quad (3.1)$$

where the low-order numerical flux  $\mathbf{g}_{i+1/2}^L = \mathbf{g}(\mathbf{v}, \mathbf{w})$  is consistent with the smooth differential flux  $\mathbf{f}(\mathbf{u}) : R^m \rightarrow R^m$  of the conservative variables  $\mathbf{u} = (u^1, \dots, u^m)^T$ .

We define the numerical entropy flux as follows.

**Definition 3.1.** *Numerical entropy flux  $G(\mathbf{v}_{i-l+1}, \dots, \mathbf{v}_{i+r})$  of the difference scheme (3.1) is called proper if for any  $\mathbf{v}_{i-l+1}, \dots, \mathbf{v}_{i+r} \in R^m$  we have*

$$\frac{\partial}{\partial v_p^j} G(\mathbf{v}_{i-l+1}, \dots, \mathbf{v}_{i+r}) = \sum_k \frac{\partial U(\mathbf{v}_p)}{\partial v_p^k} \frac{\partial}{\partial v_p^j} g^k(\mathbf{v}_{i-l+1}, \dots, \mathbf{v}_{i+r}), \quad p = i-l+1, \dots, i+r. \quad (3.2)$$

Then the proper numerical entropy flux for the difference scheme (1.8) and (1.9) can be written in the form

$$G_{i+1/2} = G_{i+1/2}^L + \alpha_{i+1/2} (G_{i+1/2}^H - G_{i+1/2}^L), \quad (3.3)$$

where  $G_{i+1/2}^L$  and  $G_{i+1/2}^H$  are the low-order and high-order proper numerical entropy fluxes corresponding to the numerical fluxes  $\mathbf{g}_{i+1/2}^L$  and  $\mathbf{g}_{i+1/2}^H$ .

**Theorem 3.1.** *Suppose that  $\mathbf{f} : R^m \rightarrow R^m$  is hemicontinuously Gateaux differentiable,  $U : R^m \rightarrow R$  is a strictly convex function with a hemicontinuous second Gateaux derivative. If matrices  $U''(\mathbf{w})g'_u(\mathbf{u}, \mathbf{v}_i)$  and  $U''(\mathbf{w})g'_u(\mathbf{v}_i, \mathbf{u})$  are positive and negative definite, respectively, for any  $\mathbf{u}, \mathbf{w} \in R^m$ ,  $\Delta t$  satisfies the inequality*

$$\begin{aligned} & \Delta t \max_{\mathbf{s} \in (\mathbf{v}_i, \hat{\mathbf{v}}_i)} \lambda(U''(\mathbf{s})) \langle (\mathbf{g}_{i+1/2}^L - \mathbf{g}_{i-1/2}^L), (\mathbf{g}_{i+1/2}^L - \mathbf{g}_{i-1/2}^L) \rangle \\ & \leq 2\Delta x [\langle U'(\mathbf{v}_i), (\mathbf{g}_{i+1/2}^L - \mathbf{g}_{i-1/2}^L) \rangle - G_{i+1/2}^L + G_{i-1/2}^L], \end{aligned} \quad (3.4)$$

then the fully discrete scheme (3.1) satisfies the discrete cell entropy inequality

$$U(\hat{\mathbf{v}}_i) - U(\mathbf{v}_i) + \frac{\Delta t}{\Delta x} [G_{i+1/2}^L(\mathbf{v}_i, \mathbf{v}_{i+1}) - G_{i-1/2}^L(\mathbf{v}_{i-1}, \mathbf{v}_i)] \leq 0. \quad (3.5)$$

where  $G_{i+1/2}^L$  is the proper numerical entropy flux corresponding to the numerical flux  $\mathbf{g}_{i+1/2}^L$ ,  $\langle \cdot, \cdot \rangle$  denotes the Euclidean inner product.

*Proof.* Multiplying (3.1) by  $U'(\mathbf{v}_i)$  and subtracting it from the left-hand side of (1.10), we get

$$\begin{aligned} & U(\hat{\mathbf{v}}_i) - U(\mathbf{v}_i) + \frac{\Delta t}{\Delta x} [G_{i+1/2}^L - G_{i-1/2}^L] \\ & = U(\hat{\mathbf{v}}_i) - U(\mathbf{v}_i) - \langle U'(\mathbf{v}_i), (\hat{\mathbf{v}}_i - \mathbf{v}_i) \rangle + \frac{\Delta t}{\Delta x} [G_{i+1/2}^L - G_{i-1/2}^L - \langle U'(\mathbf{v}_i), (\mathbf{g}_{i+1/2}^L - \mathbf{g}_{i-1/2}^L) \rangle] \\ & = \frac{1}{2} \left( \frac{\Delta t}{\Delta x} \right)^2 \langle U''(\mathbf{s}) (\mathbf{g}_{i+1/2}^L - \mathbf{g}_{i-1/2}^L), (\mathbf{g}_{i+1/2}^L - \mathbf{g}_{i-1/2}^L) \rangle \\ & \quad + \frac{\Delta t}{\Delta x} [G_{i+1/2}^L - F(\mathbf{v}_i) - \langle U'(\mathbf{v}_i), (\mathbf{g}_{i+1/2}^L - \mathbf{f}(\mathbf{v}_i)) \rangle] \\ & \quad + \frac{\Delta t}{\Delta x} [F(\mathbf{v}_i) - G_{i-1/2}^L - \langle U'(\mathbf{v}_i), (\mathbf{f}(\mathbf{v}_i) - \mathbf{g}_{i-1/2}^L) \rangle] \end{aligned} \quad (3.6)$$

where  $\mathbf{s} = \theta \hat{\mathbf{v}}_i + (1 - \theta) \mathbf{v}_i$ ,  $0 < \theta < 1$ .

It is easy to see that the first term on the right-hand side of (3.6) is non-negative. Now we show that the second and third terms in square brackets are non-positive. Indeed, we rewrite the second and third terms as follows

$$\begin{aligned} & G^L(\mathbf{v}_i, \mathbf{v}_{i+1}) - G^L(\mathbf{v}_i, \mathbf{v}_i) - \sum_j \frac{\partial U}{\partial v^j}(\mathbf{v}_i) [g^{L,j}(\mathbf{v}_i, \mathbf{v}_{i+1}) - g^{L,j}(\mathbf{v}_i, \mathbf{v}_i)] \\ &= \int_0^1 \sum_{j,k} \left[ \frac{\partial U}{\partial v^j}(\mathbf{v}_i + \xi \Delta \mathbf{v}_{i+1/2}) - \frac{\partial U}{\partial v^j}(\mathbf{v}_i) \right] \frac{\partial g^{L,j}}{\partial v^k}(\mathbf{v}_i, \mathbf{v}_i + \xi \Delta \mathbf{v}_{i+1/2}) \Delta v_{i+1/2}^k d\xi \end{aligned} \quad (3.7)$$

$$\begin{aligned} &= \int_0^1 \int_0^1 \sum_{k,l} \left[ \sum_j \frac{\partial^2 U}{\partial v^j \partial v^l}(\mathbf{v}_i + \eta \xi \Delta \mathbf{v}_{i+1/2}) \frac{\partial g^{L,j}}{\partial v^k}(\mathbf{v}_i, \mathbf{v}_i + \xi \Delta \mathbf{v}_{i+1/2}) \right] \Delta v_{i+1/2}^k \Delta v_{i+1/2}^l d\eta d\xi \\ & G^L(\mathbf{v}_i, \mathbf{v}_i) - G^L(\mathbf{v}_{i-1}, \mathbf{v}_i) - \sum_j \frac{\partial U}{\partial v^j}(\mathbf{v}_i) [g^{L,j}(\mathbf{v}_i, \mathbf{v}_i) - g^{L,j}(\mathbf{v}_{i-1}, \mathbf{v}_i)] \\ &= \int_0^1 \sum_{j,k} \left[ \frac{\partial U}{\partial v^j}(\mathbf{v}_i - \xi \Delta \mathbf{v}_{i-1/2}) - \frac{\partial U}{\partial v^j}(\mathbf{v}_i) \right] \frac{\partial g^{L,j}}{\partial v^k}(\mathbf{v}_i - \xi \Delta \mathbf{v}_{i-1/2}, \mathbf{v}_i) \Delta v_{i-1/2}^k d\xi \\ &= - \int_0^1 \int_0^1 \sum_{k,l} \left[ \sum_j \frac{\partial^2 U}{\partial v^j \partial v^l}(\mathbf{v}_i - \eta \xi \Delta \mathbf{v}_{i-1/2}) \frac{\partial g^{L,j}}{\partial v^k}(\mathbf{v}_i - \xi \Delta \mathbf{v}_{i-1/2}, \mathbf{v}_i) \right] \Delta v_{i-1/2}^k \Delta v_{i-1/2}^l d\eta d\xi \end{aligned} \quad (3.8)$$

where  $\Delta \mathbf{v}_{i+1/2} = \mathbf{v}_{i+1} - \mathbf{v}_i$ .

Thus, according to our assumption, the integrals in (3.7)-(3.8) do not change the sign over the integration interval, which means that the second and third terms are negative.

The second and third terms on the right side of (3.6) are linear in  $\Delta t$ , and the first term is of second-order. Therefore, we can choose the time step small enough that the second and third terms dominate over the first term. Consequently, the right-hand side of (3.5) is non-positive if  $\Delta t$  satisfies (3.4). This completes the proof of the theorem.  $\square$

The proper numerical entropy flux for the first-order HR scheme (2.1) can be written as follows

$$G_{i+1/2}^L = \frac{1}{2} (F(U^-) + F(U^+) - c_{i+1/2} (U^+ - U^-)). \quad (3.9)$$

Multiplying (2.1) by  $U'(\mathbf{v}_i)$  and subtracting it from the left-hand side of (1.10), we obtain

$$\begin{aligned} & U(\hat{\mathbf{v}}_i) - U(\mathbf{v}_i) + \frac{\Delta t}{\Delta x} [G_{i+1/2}^L - G_{i-1/2}^L] = U(\hat{\mathbf{v}}_i) - U(\mathbf{v}_i) - \langle U'(\mathbf{v}_i), (\hat{\mathbf{v}}_i - \mathbf{v}_i) \rangle \\ & + \frac{\Delta t}{\Delta x} \left[ G_{i+1/2}^L - G_{i-1/2}^L - \left\langle U'(\mathbf{v}_i), \left( \mathbf{g}_{i+1/2}^L - \mathbf{g}_{i-1/2}^L - \mathbf{s}_{i+1/2}^- + \mathbf{s}_{i-1/2}^+ \right) \right\rangle \right] \\ & = U(\hat{\mathbf{v}}_i) - U(\mathbf{v}_i) - \langle U'(\mathbf{v}_i), (\hat{\mathbf{v}}_i - \mathbf{v}_i) \rangle + \frac{\Delta t}{\Delta x} [\Delta G_{i+1/2}^{L,-} - \Delta G_{i-1/2}^{L,+}], \end{aligned} \quad (3.10)$$

where  $\Delta G_{i+1/2}^{L,\pm}$  are defined as

$$\begin{aligned} \Delta G_{i+1/2}^{L,\pm} &= G_{i+1/2}^L(U_{i+1/2}^-, U_{i+1/2}^+) - F(U_i) \\ &- \left\langle U'(\mathbf{v}_i), \left( \mathbf{g}_{i+1/2}^L(\mathbf{v}_{i+1/2}^-, \mathbf{v}_{i+1/2}^+) - \mathbf{s}_{i+1/2}^\pm - \mathbf{f}(\mathbf{u}_i) \right) \right\rangle. \end{aligned} \quad (3.11)$$

or substituting the values of the corresponding functions,  $\Delta G_{i+1/2}^{L,\pm}$  can be represented as

$$\begin{aligned}\Delta G_{i+1/2}^{L,-} = & \frac{1}{2} \left\{ \frac{u_{i+1}}{2} y_{i+1/2}^+ (u_{i+1} - u_i)^2 + g \left( u_{i+1} y_{i+1/2}^+ - u_i y_i \right) (z_{i+1/2} - z_i) \right. \\ & + g \left[ \frac{u_i}{2} (y_{i+1/2}^- - y_i)^2 + (y_{i+1/2}^+ - y_i) \left( u_{i+1} y_{i+1/2}^+ - \frac{u_i}{2} (y_{i+1/2}^+ + y_i) \right) \right] \\ & - c_{i+1/2} \left[ \frac{1}{2} y_{i+1/2}^+ (u_{i+1} - u_i)^2 + \frac{g}{2} (y_{i+1/2}^+ - y_i)^2 - \frac{g}{2} (y_{i+1/2}^- - y_i)^2 \right. \\ & \left. \left. + g(y_{i+1/2}^+ - y_{i+1/2}^-)(z_{i+1/2} - z_i) \right] \right\},\end{aligned}\quad (3.12)$$

$$\begin{aligned}\Delta G_{i-1/2}^{L,+} = & \frac{1}{2} \left\{ \frac{u_{i-1}}{2} y_{i-1/2}^- (u_{i-1} - u_i)^2 - g \left( u_{i-1} y_{i-1/2}^- - u_i y_i \right) (z_i - z_{i-1/2}) \right. \\ & + g \left[ \frac{u_i}{2} (y_{i-1/2}^+ - y_i)^2 + (y_{i-1/2}^- - y_i) \left( u_{i-1} y_{i-1/2}^- - \frac{u_i}{2} (y_{i-1/2}^- + y_i) \right) \right] \\ & + c_{i-1/2} \left[ \frac{1}{2} y_{i-1/2}^- (u_{i-1} - u_i)^2 - \frac{g}{2} (y_{i-1/2}^+ - y_i)^2 + \frac{g}{2} (y_{i-1/2}^- - y_i)^2 \right. \\ & \left. \left. + g(y_{i-1/2}^+ - y_{i-1/2}^-)(z_i - z_{i-1/2}) \right] \right\}.\end{aligned}\quad (3.13)$$

We consider two cases: (1) homogeneous and (2) inhomogeneous shallow water equations.

**Theorem 3.2.** Assume that  $c_{i+1/2}$  and  $\Delta t$  satisfy the inequalities

$$c_{i+1/2} \geq \frac{1}{2} \max \left( -u_{i+1} - u_i + \sqrt{(u_{i+1} - u_i)^2 + 4gy_i}, u_{i+1} + u_i + \sqrt{(u_{i+1} - u_i)^2 + 4gy_{i+1}} \right), \quad (3.14)$$

$$\begin{aligned}\Delta t \max_{\mathbf{v} \in (\mathbf{v}_i, \hat{\mathbf{v}}_i)} \lambda(U''(\mathbf{v})) \langle (\mathbf{g}_{i+1/2}^L - \mathbf{g}_{i-1/2}^L), (\mathbf{g}_{i+1/2}^L - \mathbf{g}_{i-1/2}^L) \rangle \\ \leq 2\Delta x [\langle U'(\mathbf{v}_i), (\mathbf{g}_{i+1/2}^L - \mathbf{g}_{i-1/2}^L) \rangle - G_{i+1/2}^L + G_{i-1/2}^L].\end{aligned}\quad (3.15)$$

where  $\lambda(U''(\mathbf{v})) = \frac{1}{2y}(u^2 + gy + \sqrt{(u^2 + gy)^2 - 4gy})$ .

Then for homogeneous shallow water equations, the fully discrete HR scheme (2.1)-(2.2) satisfies the discrete cell entropy inequality

$$U(\hat{\mathbf{v}}_i) - U(\mathbf{v}_i) + \frac{\Delta t}{\Delta x} [G_{i+1/2}^L(\mathbf{v}_i, \mathbf{v}_{i+1}) - G_{i-1/2}^L(\mathbf{v}_{i-1}, \mathbf{v}_i)] \leq 0. \quad (3.16)$$

where  $G_{i+1/2}^L$  is the proper numerical entropy flux (3.9).

*Proof.* For homogeneous shallow water equations, we have that  $\mathbf{v}_{i-1/2}^- = \mathbf{v}_{i-1}$ ,  $\mathbf{v}_{i+1/2}^- = \mathbf{v}_{i-1/2}^+ = \mathbf{v}_i$  and  $\mathbf{v}_{i+1/2}^+ = \mathbf{v}_{i+1}$ . Then  $\Delta G_{i+1/2}^{L,\pm}$  in (3.12)-(3.13) take the form

$$\begin{aligned}\Delta G_{i+1/2}^{L,-} = & \frac{1}{2} \left\{ \frac{u_{i+1}}{2} y_{i+1} (u_{i+1} - u_i)^2 + g(y_{i+1} - y_i) \left( u_{i+1} y_{i+1} - \frac{u_i}{2} (y_{i+1} + y_i) \right) \right. \\ & \left. - c_{i+1/2} \left[ \frac{y_{i+1}}{2} (u_{i+1} - u_i)^2 + \frac{g}{2} (y_{i+1} - y_i)^2 \right] \right\},\end{aligned}\quad (3.17)$$

$$\begin{aligned}\Delta G_{i-1/2}^{L,+} = & \frac{1}{2} \left\{ \frac{u_{i-1}}{2} y_{i-1} (u_{i-1} - u_i)^2 + g(y_{i-1} - y_i) \left( u_{i-1} y_{i-1} - \frac{u_i}{2} (y_{i-1} + y_i) \right) \right. \\ & \left. + c_{i-1/2} \left[ \frac{1}{2} y_{i-1} (u_{i-1} - u_i)^2 + \frac{g}{2} (y_{i-1} - y_i)^2 \right] \right\}.\end{aligned}\quad (3.18)$$



Note that the multipliers in the square brackets for  $c_{i\pm 1/2}$  in (3.17)-(3.18) are non-negative. It is easy to check that when they are zero, then  $\Delta G_{i\pm 1/2}^{L,\pm}$  are also zero. Let us show that  $c_{i\pm 1/2}$  can be chosen so that  $\Delta G_{i+1/2}^{L,-}$  and  $\Delta G_{i-1/2}^{L,+}$  are non-positive and non-negative, respectively. Indeed, we rewrite (3.17) as

$$\begin{aligned}\Delta G_{i+1/2}^{L,-} &= \frac{1}{2} \left\{ \frac{u_{i+1}}{2} y_{i+1} (u_{i+1} - u_i)^2 + g y_{i+1} (y_{i+1} - y_i) (u_{i+1} - u_i) \right. \\ &\quad \left. + g \frac{u_i}{2} (y_{i+1} - y_i)^2 - c_{i+1/2} \left[ \frac{y_{i+1}}{2} (u_{i+1} - u_i)^2 + \frac{g}{2} (y_{i+1} - y_i)^2 \right] \right\} \\ &= \frac{1}{2} \left\{ \frac{y_{i+1}}{2} (u_{i+1} - c_{i+1/2}) (u_{i+1} - u_i)^2 + g y_{i+1} (y_{i+1} - y_i) (u_{i+1} - u_i) \right. \\ &\quad \left. + \frac{g}{2} (u_i - c_{i+1/2}) (y_{i+1} - y_i)^2 \right\}.\end{aligned}\tag{3.19}$$

$\Delta G_{i+1/2}^{L,-}$  is a quadratic form with respect to  $(u_{i+1} - u_i)$  and  $(y_{i+1} - y_i)$ . For it to be non-positive, it is sufficient for the leading coefficient and its discriminant to be non-positive. Then,  $c_{i+1/2}$  should satisfy the following inequalities

$$\begin{aligned}c_{i+1/2} - u_{i+1} &> 0, \\ c_{i+1/2}^2 - (u_{i+1} + u_i) c_{i+1/2} + u_{i+1} u_i - g y_{i+1} &\geq 0.\end{aligned}\tag{3.20}$$

It is clear that inequalities (3.20) hold for  $c_{i+1/2} \geq \frac{1}{2} (u_{i+1} + u_i + \sqrt{(u_{i+1} - u_i)^2 + 4g y_{i+1}})$ . Similarly, it can be shown that  $\Delta G_{i-1/2}^{L,+}$  is non-negative for  $c_{i-1/2} \geq \frac{1}{2} (-u_{i-1} - u_i + \sqrt{(u_{i-1} - u_i)^2 + 4g y_{i-1}})$ .

We rewrite the discrete cell entropy inequality (3.10) in the form

$$\begin{aligned}U(\hat{\mathbf{v}}_i) - U(\mathbf{v}_i) + \frac{\Delta t}{\Delta x} [G_{i+1/2}^L - G_{i-1/2}^L] \\ = U(\hat{\mathbf{v}}_i) - U(\mathbf{v}_i) - \langle U'(\mathbf{v}_i), (\hat{\mathbf{v}}_i - \mathbf{v}_i) \rangle + \frac{\Delta t}{\Delta x} [\Delta G_{i+1/2}^{L,-} - \Delta G_{i-1/2}^{L,+}] \\ = \frac{1}{2} \left( \frac{\Delta t}{\Delta x} \right)^2 \langle U''(\mathbf{s}) (\mathbf{g}_{i+1/2}^L - \mathbf{g}_{i-1/2}^L), (\mathbf{g}_{i+1/2}^L - \mathbf{g}_{i-1/2}^L) \rangle + \frac{\Delta t}{\Delta x} [\Delta G_{i+1/2}^{L,-} - \Delta G_{i-1/2}^{L,+}].\end{aligned}\tag{3.21}$$

Thus, the non-positivity of (3.21) can be achieved by choosing a sufficiently small  $\Delta t$  so that the second term dominates over the first non-negative term on the right-hand side of (3.21). This completes the proof of the theorem.  $\square$

**Theorem 3.3.** Suppose that  $c_{i+1/2}$  and  $\Delta t$  satisfy the inequalities

$$\begin{aligned}c_{i+1/2} \geq \max \left( \frac{a_i^- u_{i+1} + b_i^- u_i + \sqrt{(a_i^- u_{i+1} - b_i^- u_i)^2 + 4g a_i^- y_{i+1/2}^+ (w_{i+1/2}^+ - w_i)^2}}{2a_i^-}, \right. \\ \left. \frac{-a_{i+1}^+ u_i - b_{i+1}^+ u_{i+1} + \sqrt{(a_{i+1}^+ u_i - b_{i+1}^+ u_{i+1})^2 + 4g a_{i+1}^+ y_{i+1/2}^- (w_{i+1/2}^- - w_{i+1})^2}}{2a_{i+1}^+} \right).\end{aligned}\tag{3.22}$$

$$\begin{aligned}\Delta t \max_{\mathbf{v} \in (\mathbf{v}_i, \hat{\mathbf{v}}_i)} \lambda(U''(\mathbf{v})) \langle (\mathbf{g}_{i+1/2}^L - \mathbf{g}_{i-1/2}^L - \mathbf{s}_{i+1/2}^- + \mathbf{s}_{i-1/2}^+), (\mathbf{g}_{i+1/2}^L - \mathbf{g}_{i-1/2}^L - \mathbf{s}_{i+1/2}^- + \mathbf{s}_{i-1/2}^+) \rangle \\ \leq 2\Delta x \left[ \langle U'(\mathbf{v}_i), (\mathbf{g}_{i+1/2}^L - \mathbf{g}_{i-1/2}^L - \mathbf{s}_{i+1/2}^- + \mathbf{s}_{i-1/2}^+) \rangle - G_{i+1/2}^L + G_{i-1/2}^L \right].\end{aligned}\tag{3.23}$$

where

$$\begin{aligned}\lambda(U''(\mathbf{v})) &= \frac{1}{2y}(u^2 + gy + \sqrt{(u^2 + gy)^2 - 4gy}) \\ a_i^\mp &= \pm(y_{i\pm 1/2}^+ - y_{i\pm 1/2}^-) \left( w_{i\pm 1/2}^\pm + w_{i\pm 1/2}^- - 2w_i \right), \\ b_i^\mp &= \pm(y_{i\pm 1/2}^- - y_i)^2 \mp (y_{i\pm 1/2}^+ - y_i)^2 + 2(y_{i\pm 1/2}^\pm - y_i)(w_{i\pm 1/2}^\pm - w_i).\end{aligned}\tag{3.24}$$

Then for inhomogeneous shallow water equations, the fully discrete HR scheme (2.1)-(2.2) satisfies the discrete cell entropy inequality

$$U(\hat{\mathbf{v}}_i) - U(\mathbf{v}_i) + \frac{\Delta t}{\Delta x} \left[ G_{i+1/2}^L(\mathbf{v}_{i+1/2}^-, \mathbf{v}_{i+1/2}^+) - G_{i-1/2}^L(\mathbf{v}_{i-1/2}^-, \mathbf{v}_{i-1/2}^+) \right] \leq 0.\tag{3.25}$$

where  $G_{i+1/2}^L$  is the proper numerical entropy flux (3.9).

*Proof.* We rewrite  $\Delta G_{i+1/2}^{L,\pm}$  in (3.12)-(3.13) as follows

$$\begin{aligned}\Delta G_{i+1/2}^{L,-} &= \frac{1}{2} \left\{ \frac{u_{i+1}}{2} y_{i+1/2}^+ (u_{i+1} - u_i)^2 + g y_{i+1/2}^+ (u_{i+1} - u_i) (w_{i+1/2}^+ - w_i) \right. \\ &\quad + g \left[ \frac{u_i}{2} (y_{i+1/2}^- - y_i)^2 - \frac{u_i}{2} (y_{i+1/2}^+ - y_i)^2 + u_i (y_{i+1/2}^+ - y_i) (w_{i+1/2}^+ - w_i) \right] \\ &\quad \left. - c_{i+1/2} \left[ \frac{1}{2} y_{i+1/2}^+ (u_{i+1} - u_i)^2 + g (y_{i+1/2}^+ - y_{i+1/2}^-) \left( \frac{1}{2} (w_{i+1/2}^+ + w_{i+1/2}^-) - w_i \right) \right] \right\},\end{aligned}\tag{3.26}$$

$$\begin{aligned}\Delta G_{i-1/2}^{L,+} &= \frac{1}{2} \left\{ \frac{u_{i-1}}{2} y_{i-1/2}^- (u_{i-1} - u_i)^2 - g y_{i-1/2}^- (u_{i-1} - u_i) (w_i - w_{i-1/2}^-) \right. \\ &\quad + g \left[ \frac{u_i}{2} (y_{i-1/2}^+ - y_i)^2 - \frac{u_i}{2} (y_{i-1/2}^- - y_i)^2 + u_i (y_{i-1/2}^- - y_i) (w_{i-1/2}^- - w_i) \right] \\ &\quad \left. + c_{i-1/2} \left[ \frac{1}{2} y_{i-1/2}^- (u_{i-1} - u_i)^2 + g (y_{i-1/2}^+ - y_{i-1/2}^-) \left( w_i - \frac{1}{2} (w_{i-1/2}^+ + w_{i-1/2}^-) \right) \right] \right\}.\end{aligned}\tag{3.27}$$

Let us show that the coefficients in the square brackets at  $c_{i\pm 1/2}$  in (3.26)-(3.27) are non-negative. Consider the following cases:

(i) In the fully wet case,  $\min(w_i, w_{i+1}) > \max(z_i, z_{i+1})$ . According to (2.4)-(2.5), we have  $w_{i+1/2}^- = w_i$  and  $w_{i+1/2}^+ = w_{i+1}$ .

Hence, if  $y_{i+1/2}^+ \geq y_{i+1/2}^-$ , then  $w_{i+1/2}^+ \geq w_{i+1/2}^-$ , and  $(y_{i+1/2}^+ - y_{i+1/2}^-) \left( \frac{1}{2} (w_{i+1/2}^+ + w_{i+1/2}^-) - w_i \right) \geq 0$ . Otherwise, if  $y_{i+1/2}^+ < y_{i+1/2}^-$ , then also  $w_{i+1/2}^+ < w_{i+1/2}^-$ , and the required inequality holds.

(ii) In the partially wet case  $\min(w_i, w_{i+1}) \leq \max(z_i, z_{i+1})$ . Depending on which bottom is higher, right or left, we consider two subcases.

Let  $z_i \geq z_{i+1}$ . Then  $z_{i+1/2} = w_{i+1}$ ,  $y_{i+1/2}^- = y_i$ ,  $y_{i+1/2}^+ = 0$ , and  $w_{i+1/2}^-, w_{i+1/2}^+ \leq w_i$ . Therefore,  $(y_{i+1/2}^+ - y_{i+1/2}^-) \left( \frac{1}{2} (w_{i+1/2}^+ + w_{i+1/2}^-) - w_i \right) \geq 0$ .

If  $z_i < z_{i+1}$ , then  $z_{i+1/2} = w_i$ ,  $y_{i+1/2}^- = 0$ ,  $y_{i+1/2}^+ = y_{i+1}$ , and  $w_{i+1/2}^- = w_i$ ,  $w_{i+1/2}^+ > w_i$ . Thus, we again obtain the required inequality.

The non-negativity of the terms in square brackets at  $c_{i-1/2}$  is proved similarly.

It is easy to check that when they are zero, then  $\Delta G_{i\mp 1/2}^{L,\pm}$  are also zero. Let us show that  $c_{i\pm 1/2}$  can be chosen so that  $\Delta G_{i+1/2}^{L,-}$  and  $\Delta G_{i-1/2}^{L,+}$  are non-positive and non-negative, respectively. Indeed, we consider  $\Delta G_{i+1/2}^{L,-}$  and  $\Delta G_{i-1/2}^{L,+}$  as quadratic equations with respect to  $(u_{i+1} - u_i)$  and  $(u_{i-1} - u_i)$ , respectively.

$\Delta G_{i+1/2}^{L,-}$  will be non-positive if its leading coefficient and discriminant are non-positive, i.e.

$$\begin{aligned} c_{i+1/2} &> u_{i+1}, \\ -a_i^- c_{i+1/2}^2 + (a_i^- u_{i+1} + b_i^- u_i) c_{i+1/2} - u_{i+1} u_i b_i^- + g y_{i+1/2}^+ (w_{i+1/2}^+ - w_i)^2 &\leq 0, \end{aligned} \quad (3.28)$$

where

$$\begin{aligned} a_i^- &= (y_{i+1/2}^+ - y_{i+1/2}^-) (w_{i+1/2}^+ + w_{i+1/2}^- - 2w_i), \\ b_i^- &= (y_{i+1/2}^- - y_i)^2 - (y_{i+1/2}^+ - y_i)^2 + 2(y_{i+1/2}^+ - y_i)(w_{i+1/2}^+ - w_i). \end{aligned} \quad (3.29)$$

It is clear that the inequalities (3.28) hold for

$$c_{i+1/2} \geq \frac{a_i^- u_{i+1} + b_i^- u_i + \sqrt{(a_i^- u_{i+1} - b_i^- u_i)^2 + 4g a_i^- y_{i+1/2}^+ (w_{i+1/2}^+ - w_i)^2}}{2a_i^-}. \quad (3.30)$$

Similarly, it is proved that  $\Delta G_{i-1/2}^{L,+}$  is non-negative for

$$c_{i-1/2} \geq \frac{-a_i^+ u_{i-1} - b_i^+ u_i + \sqrt{(a_i^+ u_{i-1} - b_i^+ u_i)^2 + 4g a_i^+ y_{i-1/2}^- (w_{i-1/2}^- - w_i)^2}}{2a_i^+}, \quad (3.31)$$

where

$$\begin{aligned} a_i^+ &= (y_{i-1/2}^+ - y_{i-1/2}^-) (2w_i - w_{i-1/2}^+ - w_{i-1/2}^-), \\ b_i^+ &= (y_{i-1/2}^+ - y_i)^2 - (y_{i-1/2}^- - y_i)^2 + 2(y_{i-1/2}^- - y_i)(w_{i-1/2}^- - w_i). \end{aligned} \quad (3.32)$$

Thus, returning to the discrete entropy inequality (3.21), we can choose  $\Delta t$  so that the non-positive terms in square brackets dominate over the non-negative first term on the right-hand side of (3.21). This concludes the proof of the theorem.  $\square$

## 4 Finding Flux Limiters

The system of equations (1.8)-(1.9) is nonlinear if we consider  $\alpha$  as a function of  $\hat{\mathbf{v}}$ , and it can be written in the form

$$\hat{\mathbf{v}} - \Delta t P \hat{\mathbf{v}} = \hat{\mathbf{v}}^L, \quad (4.1)$$

where mapping  $P : R^N \times R^N \rightarrow R^N \times R^N$  is defined by  $P_i \hat{\mathbf{v}} = \left[ \alpha_{i-1/2}(\hat{\mathbf{v}}) \mathbf{g}_{i-1/2}^{AD} - \alpha_{i+1/2}(\hat{\mathbf{v}}) \mathbf{g}_{i+1/2}^{AD} \right] / \Delta x$ ,  $\mathbf{g}_{i+1/2}^{AD} = \mathbf{g}_{i+1/2}^H - \mathbf{g}_{i+1/2}^L$ , and  $\hat{\mathbf{v}}_i^L = \mathbf{v}_i - \Delta t / \Delta x (\mathbf{g}_{i+1/2}^L - \mathbf{g}_{i-1/2}^L) + \mathbf{s}_i$ . Let  $O_0 = \bar{O}(\hat{\mathbf{v}}^L, \delta)$  be a closed ball with center at  $\hat{\mathbf{v}}^L$  and radius  $\delta > 0$ . Furthermore, we define a mapping  $S\mathbf{v} : O_0 \rightarrow R^N \times R^N$  as

$$S\mathbf{v} = \mathbf{v} - \Delta t P \mathbf{v}. \quad (4.2)$$

Let us show that for sufficiently small  $\Delta t$  the system of equations (4.1) is uniquely solvable in a neighborhood of the first-order HR solution of (2.1).

**Theorem 4.1.** *Assume that*

$$\|P(\mathbf{w}) - P(\mathbf{v})\| \leq M\|\mathbf{w} - \mathbf{v}\|, \quad \forall \mathbf{v}, \mathbf{w} \in O_0. \quad (4.3)$$

*If  $\Delta t$  satisfies*

$$\Delta t < \delta(\|P\hat{\mathbf{v}}^L\| + \delta M)^{-1}, \quad (4.4)$$

*then the system of equations (4.1) has a unique solution in  $O_0$ .*

*Proof.* Our proof mimics the proof of theorem 5.1.6 [24, p.122]. For fixed  $\mathbf{d} \in O(S\hat{\mathbf{v}}^L, \varepsilon)$ , we define the mapping  $T : O_0 \rightarrow R^N \times R^N$  by

$$T\mathbf{y} = \Delta t P\mathbf{v} + \mathbf{d} = \mathbf{v} - [S\mathbf{v} - \mathbf{d}].$$

Then,  $S\mathbf{v} = \mathbf{d}$  has a unique solution in  $O_0$  if and only if  $T$  has a unique fixed point. For any  $\mathbf{v}, \mathbf{w} \in O_0$

$$\|T\mathbf{v} - T\mathbf{w}\| = \Delta t\|P\mathbf{v} - P\mathbf{w}\| \leq \Delta t M \|\mathbf{v} - \mathbf{w}\| \quad (4.5)$$

and  $S$  is contractive on  $O_0$  if  $\Delta t M < 1$ . Moreover, for any  $\mathbf{v} \in O_0$ ,

$$\|T\mathbf{v} - \hat{\mathbf{v}}^L\| \leq \|T\mathbf{v} - T\hat{\mathbf{v}}^L\| + \|T\hat{\mathbf{v}}^L - \hat{\mathbf{v}}^L\| \leq \Delta t M \|\mathbf{v} - \hat{\mathbf{v}}^L\| + \|S\mathbf{v} - \mathbf{d}\| \leq \Delta t M \delta + \varepsilon. \quad (4.6)$$

For  $\varepsilon = \delta(1 - \Delta t M)$ , the expression on the right-hand side of (4.6) equal to  $\delta$ . Hence,  $T$  maps  $O_0$  into  $O_0$ , and for any  $\mathbf{d} \in O(S\hat{\mathbf{v}}^L, \varepsilon)$  the equation  $S\mathbf{v} = \mathbf{d}$  has a unique solution in  $O_0$ .

Finally, we have that  $\hat{\mathbf{v}}^L \in O(S\hat{\mathbf{v}}^L, \varepsilon)$  if

$$\|S\hat{\mathbf{v}}^L - \hat{\mathbf{v}}^L\| = \Delta t\|P\hat{\mathbf{v}}^L\| < \varepsilon. \quad (4.7)$$

Combining all restrictions on  $\Delta t$ , we obtain that the nonlinear system of equation (4.1) has a unique solution if  $\Delta t$  satisfies (4.4).  $\square$

**Remark 4.1.** *Note that the mapping  $S$  in (4.2) is contractive in the vicinity of a low-order solution with the HR scheme (2.1)-(2.7) if the mapping  $P$  in (4.1) is Lipschitz-continuous.*

Our goal is to find the maximum values of the flux limiters  $\boldsymbol{\alpha} \in U_{ad} = \{\boldsymbol{\alpha} \mid 0 \leq \alpha_{i+1/2} \leq 1\}$ , for which the numerical solution of the hybrid scheme (1.8)-(1.9) satisfies the constraints (2.9)-(2.10) and the discrete cell entropy inequality (3.25). Then finding the flux limiters can be considered as the following optimization problem

$$\mathfrak{F}(\boldsymbol{\alpha}) = \sum_i \alpha_{i+1/2} \rightarrow \max_{\boldsymbol{\alpha} \in U_{ad}} \quad (4.8)$$

subject to

$$\begin{aligned} \frac{\Delta x}{\Delta t} (\underline{w}_i - w_i) + \frac{c_{i+1/2} - u_{i+1}}{2} (w_i - w_{i+1/2}^+) + \frac{c_{i-1/2} + u_{i-1}}{2} (w_i - w_{i-1/2}^-) &\leq -\alpha_{i+1/2} g_{i+1/2}^{AD,y} \\ + \alpha_{i-1/2} g_{i-1/2}^{AD,y} &\leq \frac{\Delta x}{\Delta t} (\bar{w}_i - w_i) + \frac{c_{i+1/2} - u_{i+1}}{2} (w_i - w_{i+1/2}^+) + \frac{c_{i-1/2} + u_{i-1}}{2} (w_i - w_{i-1/2}^-), \end{aligned} \quad (4.9)$$

$$\begin{aligned} & \frac{\Delta x}{\Delta t} \left( \underline{q}_i - q_i \right) + \frac{c_{i+1/2} - u_{i+1}}{2} (q_i - q_{i+1/2}^+) + \frac{c_{i-1/2} + u_{i-1}}{2} (q_i - q_{i-1/2}^-) \leq -\alpha_{i+1/2} g_{i+1/2}^{AD,q} \\ & + \alpha_{i-1/2} g_{i-1/2}^{AD,q} \leq \frac{\Delta x}{\Delta t} (\bar{q}_i - q_i) + \frac{c_{i+1/2} - u_{i+1}}{2} (q_i - q_{i+1/2}^+) + \frac{c_{i-1/2} + u_{i-1}}{2} (q_i - q_{i-1/2}^-), \end{aligned} \quad (4.10)$$

$$\begin{aligned} & \frac{\Delta x}{\Delta t} [U(\hat{\mathbf{v}}_i) - U(\mathbf{v}_i) - \langle U'(\mathbf{v}_i), (\hat{\mathbf{v}}_i - \mathbf{v}_i) \rangle] - \left\langle U'(\mathbf{v}_i), (\mathbf{g}_{i+1/2}^L - \mathbf{g}_{i-1/2}^L - \mathbf{s}_{i+1/2}^- + \mathbf{s}_{i-1/2}^+) \right\rangle \\ & + G_{i+1/2}^L - G_{i-1/2}^L \leq \alpha_{i+1/2} (\langle U'(\mathbf{v}_i), \mathbf{g}_{i+1/2}^{AD} \rangle - G_{i+1/2}^{AD}) - \alpha_{i-1/2} (\langle U'(\mathbf{v}_i), \mathbf{g}_{i-1/2}^{AD} \rangle - G_{i-1/2}^{AD}), \end{aligned} \quad (4.11)$$

$$\frac{\Delta x}{\Delta t} (\hat{\mathbf{v}}_i - \mathbf{v}_i) + \mathbf{g}_{i+1/2}^L - \mathbf{g}_{i-1/2}^L - \mathbf{s}_{i+1/2}^- + \mathbf{s}_{i-1/2}^+ + \alpha_{i+1/2} \mathbf{g}_{i+1/2}^{AD} - \alpha_{i-1/2} \mathbf{g}_{i-1/2}^{AD} = 0, \quad (4.12)$$

where  $\underline{w}_i = \min(w_i, w_{i-1/2}^-, w_{i+1/2}^+)$ ,  $\bar{w}_i = \max(w_i, w_{i-1/2}^-, w_{i+1/2}^+)$ , and  $G_{i+1/2}^{AD} = G_{i+1/2}^H - G_{i+1/2}^L$ .

Due to constraints (4.11) the optimization problem (4.8)-(4.12) is nonlinear. Consequently, finding a numerical entropy solution of shallow water equations with variable bottom topography (1.1)-(1.2) in one time step can be represented as the following iterative process.

*Step 1.* Initialize positive numbers  $\delta$ ,  $\epsilon_1$ , and  $\epsilon_2$ . Set  $p = 0$ ,  $\hat{\mathbf{v}}^0 = \mathbf{v}$ ,  $\boldsymbol{\alpha}^0 = 0$ .

*Step 2.* Find  $\boldsymbol{\alpha}^{p+1}$  as a solution to the following linear programming problem

$$\mathfrak{S}(\boldsymbol{\alpha}) = \sum_i \alpha_{i+1/2}^{p+1} \rightarrow \max_{\boldsymbol{\alpha}^{p+1} \in U_{ad}} \quad (4.13)$$

subject to

$$\begin{aligned} & \frac{\Delta x}{\Delta t} (\underline{w}_i - w_i) + \frac{c_{i+1/2} - u_{i+1}}{2} (w_i - w_{i+1/2}^+) + \frac{c_{i-1/2} + u_{i-1}}{2} (w_i - w_{i-1/2}^-) \leq -\alpha_{i+1/2}^{p+1} g_{i+1/2}^{AD,y} \\ & + \alpha_{i-1/2}^{p+1} g_{i-1/2}^{AD,y} \leq \frac{\Delta x}{\Delta t} (\bar{w}_i - w_i) + \frac{c_{i+1/2} - u_{i+1}}{2} (w_i - w_{i+1/2}^+) + \frac{c_{i-1/2} + u_{i-1}}{2} (w_i - w_{i-1/2}^-), \end{aligned} \quad (4.14)$$

$$\begin{aligned} & \frac{\Delta x}{\Delta t} \left( \underline{q}_i - q_i \right) + \frac{c_{i+1/2} - u_{i+1}}{2} (q_i - q_{i+1/2}^+) + \frac{c_{i-1/2} + u_{i-1}}{2} (q_i - q_{i-1/2}^-) \leq -\alpha_{i+1/2}^{p+1} g_{i+1/2}^{AD,q} \\ & + \alpha_{i-1/2}^{p+1} g_{i-1/2}^{AD,q} \leq \frac{\Delta x}{\Delta t} (\bar{q}_i - q_i) + \frac{c_{i+1/2} - u_{i+1}}{2} (q_i - q_{i+1/2}^+) + \frac{c_{i-1/2} + u_{i-1}}{2} (q_i - q_{i-1/2}^-), \end{aligned} \quad (4.15)$$

$$\begin{aligned} & \frac{\Delta x}{\Delta t} [U(\hat{\mathbf{v}}_i^p) - U(\mathbf{v}_i) - \langle U'(\mathbf{v}_i), (\hat{\mathbf{v}}_i^p - \mathbf{v}_i) \rangle] - \left\langle U'(\mathbf{v}_i), (\mathbf{g}_{i+1/2}^L - \mathbf{g}_{i-1/2}^L - \mathbf{s}_{i+1/2}^- + \mathbf{s}_{i-1/2}^+) \right\rangle \\ & + G_{i+1/2}^L - G_{i-1/2}^L \leq \alpha_{i+1/2}^{p+1} (\langle U'(\mathbf{v}_i), \mathbf{g}_{i+1/2}^{AD} \rangle - G_{i+1/2}^{AD}) - \alpha_{i-1/2}^{p+1} (\langle U'(\mathbf{v}_i), \mathbf{g}_{i-1/2}^{AD} \rangle - G_{i-1/2}^{AD}), \end{aligned} \quad (4.16)$$

Step 3. For  $\alpha^{p+1}$  we find  $\hat{\mathbf{v}}^{p+1}$  from the system of linear equations

$$\frac{\Delta x}{\Delta t} (\hat{\mathbf{v}}_i^{p+1} - \mathbf{v}_i) + \mathbf{g}_{i+1/2}^L - \mathbf{g}_{i-1/2}^L - \mathbf{s}_{i+1/2}^- + \mathbf{s}_{i-1/2}^+ + \alpha_{i+1/2}^{p+1} \mathbf{g}_{i+1/2}^{AD} - \alpha_{i-1/2}^{p+1} \mathbf{g}_{i-1/2}^{AD} = 0, \quad (4.17)$$

Step 4. Algorithm stop criterion

$$\frac{|\hat{y}_i^{p+1} - \hat{y}_i^p|}{\max(\delta, |\hat{y}_i^{p+1}|)} < \varepsilon_1, \quad \frac{|\hat{q}_i^{p+1} - \hat{q}_i^p|}{\max(\delta, |\hat{q}_i^{p+1}|)} < \varepsilon_1, \quad \left| \alpha_{i+1/2}^{p+1} - \alpha_{i+1/2}^p \right| < \varepsilon_2. \quad (4.18)$$

If conditions (4.18) hold, then set  $\hat{\mathbf{v}} = \hat{\mathbf{v}}^{p+1}$ . Otherwise, set  $p = p + 1$  and go to Step 2.

**Remark 4.2.** It is clear that the linear programming problem (4.13)-(4.16) is solvable if  $\Delta t$  satisfies inequalities (2.8) and (3.23). It follows from the non-emptiness of the feasible set and the boundedness on  $U_{ad}$  of the objective function  $\mathfrak{S}(\alpha)$ .

## 5 Approximate Solution to the Optimization Problem

Solving a linear programming problem is computationally expensive. So, at Step 2, instead of solving the linear programming problem, it is reasonable to use its computationally less expensive approximate solution. In this section our goal is to look for an approximate solution of the linear programming problem (4.13) - (4.16).

First, we find a nontrivial  $\alpha \in U_{ad}$  satisfying inequalities (4.14), which are rewritten in the form

$$-\alpha_{i+1/2} g_{i+1/2}^{AD,y} + \alpha_{i-1/2} g_{i-1/2}^{AD,y} \geq Q_i^{-,y}, \quad (5.1)$$

$$-\alpha_{i+1/2} g_{i+1/2}^{AD,y} + \alpha_{i-1/2} g_{i-1/2}^{AD,y} \leq Q_i^{+,y}, \quad (5.2)$$

where

$$Q_i^{+,y} = \frac{\Delta x}{\Delta t} (\bar{w}_i - w_i) + \frac{c_{i+1/2} - u_{i+1}}{2} (w_i - w_{i+1/2}^+) + \frac{c_{i-1/2} + u_{i-1}}{2} (w_i - w_{i-1/2}^-),$$

$$Q_i^{-,y} = \frac{\Delta x}{\Delta t} (\underline{w}_i - w_i) + \frac{c_{i+1/2} - u_{i+1}}{2} (w_i - w_{i+1/2}^+) + \frac{c_{i-1/2} + u_{i-1}}{2} (w_i - w_{i-1/2}^-).$$

Denote by  $\alpha_i^{-,y}$  and  $\alpha_i^{+,y}$  the maximum values of the components  $\alpha$  for the negative and positive terms on the left-hand side of (5.1)-(5.2), respectively. Then

$$-\alpha_{i+1/2} g_{i+1/2}^{AD,y} + \alpha_{i-1/2} g_{i-1/2}^{AD,y} \geq \alpha_i^{-,y} P_i^{-,y}, \quad (5.3)$$

$$-\alpha_{i+1/2} g_{i+1/2}^{AD,y} + \alpha_{i-1/2} g_{i-1/2}^{AD,y} \leq \alpha_i^{+,y} P_i^{+,y}, \quad (5.4)$$

where

$$P_i^{-,y} = \min \left( 0, -g_{i+1/2}^{AD,y} \right) + \min \left( 0, g_{i-1/2}^{AD,y} \right),$$

$$P_i^{+,y} = \max \left( 0, -g_{i+1/2}^{AD,y} \right) + \max \left( 0, g_{i-1/2}^{AD,y} \right).$$

Each flux limiter  $\alpha_{i+1/2}$  appears twice in (5.3) and twice in (5.4) with coefficients that differ only in sign. Substituting (5.3)-(5.4) into (5.1)-(5.2), we obtain that  $\alpha_{i+1/2}$  should not exceed

$$\bar{\alpha}_{i+1/2}^y = \begin{cases} \min(\alpha_i^{+,y}, \alpha_{i+1}^{-,y}) = \min(R_i^{+,y}, R_{i+1}^{-,y}), & g_{i+1/2}^{AD,y} < 0, \\ \min(\alpha_i^{-,y}, \alpha_{i+1}^{+,y}) = \min(R_i^{-,y}, R_{i+1}^{+,y}), & g_{i+1/2}^{AD,y} > 0, \end{cases} \quad (5.5)$$

where  $R_i^{-,y} = \min(1, \min(0, Q_i^{-,y})/P_i^{-,y})$  and  $R_i^{+,y} = \min(1, \max(0, Q_i^{+,y})/P_i^{+,y})$ .

Similarly, it is proved that inequalities (4.15) hold for

$$\bar{\alpha}_{i+1/2}^q = \begin{cases} \min(\alpha_i^{+,q}, \alpha_{i+1}^{-,q}) = \min(R_i^{+,q}, R_{i+1}^{-,q}), & g_{i+1/2}^{AD,q} < 0, \\ \min(\alpha_i^{-,q}, \alpha_{i+1}^{+,q}) = \min(R_i^{-,q}, R_{i+1}^{+,q}), & g_{i+1/2}^{AD,q} > 0, \end{cases} \quad (5.6)$$

where  $R_i^{-,q} = \min(1, \min(0, Q_i^{-,q})/P_i^{-,q})$  and  $R_i^{+,q} = \min(1, \max(0, Q_i^{+,q})/P_i^{+,q})$ ,

$$Q_i^{+,q} = \frac{\Delta x}{\Delta t} (\bar{q}_i - q_i) + \frac{c_{i+1/2} - u_{i+1}}{2} (q_i - q_{i+1/2}^+) + \frac{c_{i-1/2} + u_{i-1}}{2} (q_i - q_{i-1/2}^-),$$

$$Q_i^{-,q} = \frac{\Delta x}{\Delta t} (\underline{q}_i - q_i) + \frac{c_{i+1/2} - u_{i+1}}{2} (q_i - q_{i+1/2}^+) + \frac{c_{i-1/2} + u_{i-1}}{2} (q_i - q_{i-1/2}^-).$$

$$P_i^{-,q} = \min(0, -g_{i+1/2}^{AD,q}) + \min(0, g_{i-1/2}^{AD,q}),$$

$$P_i^{+,q} = \max(0, -g_{i+1/2}^{AD,q}) + \max(0, g_{i-1/2}^{AD,q}).$$

Finally, we rewrite (4.16) in the form

$$A_i \leq \alpha_{i+1/2} d_{ii+1} + \alpha_{i-1/2} d_{ii-1}, \quad (5.7)$$

where

$$A_i = \frac{\Delta x}{\Delta t} (U(\hat{\mathbf{v}}_i) - U(\mathbf{v}_i) - \langle U'(\mathbf{v}_i), (\hat{\mathbf{v}}_i - \mathbf{v}_i) \rangle) + G_{i+1/2}^L - G_{i-1/2}^L$$

$$- \langle U'(\mathbf{v}_i), (\mathbf{g}_{i+1/2}^L - \mathbf{g}_{i-1/2}^L - \mathbf{s}_{i+1/2}^- + \mathbf{s}_{i-1/2}^+) \rangle,$$

$$d_{ik} = (\langle U'(\mathbf{v}_i), \mathbf{g}_{(i+k)/2}^{AD} \rangle - G_{(i+k)/2}^{AD}) \operatorname{sgn}(k - i).$$

By reasoning similar to the above, we obtain from (5.7) that the upper bound of  $\alpha_{i+1/2}$  is equal to

$$\bar{\alpha}_{i+1/2}^U = \min \left\{ 1, \frac{-A_i}{B_i} \min(0, \operatorname{sgn} d_{ii+1}) + \max(0, \operatorname{sgn} d_{ii+1}), \right. \\ \left. \frac{-A_{i+1}}{B_{i+1}} \min(0, \operatorname{sgn} d_{i+1i}) + \max(0, \operatorname{sgn} d_{i+1i}) \right\}, \quad (5.8)$$

where  $B_i = \min(0, d_{ii+1}) + \min(0, d_{ii-1})$

Thus, a nontrivial feasible solution to the linear programming problem (4.13)-(4.16) on  $U_{ad}$  is equal to

$$\alpha_{i+1/2} = \min(\bar{\alpha}_{i+1/2}^y, \bar{\alpha}_{i+1/2}^q, \bar{\alpha}_{i+1/2}^U). \quad (5.9)$$

**Theorem 5.1.** *Let  $U(\hat{\mathbf{v}}) : R^N \times R^N \rightarrow R^N \times R^N$  be a Lipschitz-continuous function on a closed ball  $O_0 = \bar{O}(\hat{\mathbf{v}}^L, \delta)$ , where  $\hat{\mathbf{v}}^L$  is a solution of the system of equations (2.1). Then the flux limiters  $\alpha$ , defined by (5.9), are Lipschitz-continuous on  $O_0$ .*

*Proof.* It is clear that  $\bar{\alpha}_{i+1/2}^y, \bar{\alpha}_{i+1/2}^q, B_i, d_{ik}$  are constants, and  $A_i$  are Lipschitz-continuous functions on  $O_0$ . Thus,  $\alpha_{i+1/2}, \bar{\alpha}_{i+1/2}^U$  are Lipschitz-continuous on  $O_0$ , since the minimum of Lipschitz-continuous functions is again a Lipschitz-continuous function.  $\square$

**Remark 5.1.** *The hypotheses of Theorems 4.1 and 5.1 are satisfied if  $U(\mathbf{v})$  is a strictly convex function, and  $\alpha_{i+1/2}$  are calculated using (5.1)-(5.9). In this case, the system of equations (4.1) has a unique solution.*

**Remark 5.2.** *The approach presented in this paper can be extended to multidimensional and implicit HR schemes. For details we refer the reader to [15].*

## 6 Numerical Examples

In this section, we demonstrate the benefits of the proposed approach and compare numerical results with analytical and previous numerical studies. We also compare numerical results obtained with flux limiters, which are approximate and exact solutions to the corresponding optimization problems.

Applying the centered space flux as a high-order flux, we use the following hybrid HR scheme in our calculations

$$\begin{aligned} \hat{\mathbf{v}}_i - \mathbf{v}_i + \frac{\Delta t}{\Delta x} \left[ \mathbf{g}_{i+1/2}^L(\mathbf{v}_{i+1/2}^-, \mathbf{v}_{i+1/2}^+) - \mathbf{g}_{i-1/2}^L(\mathbf{v}_{i-1/2}^-, \mathbf{v}_{i+1/2}^+) \right] \\ + \frac{1}{2} \frac{\Delta t}{\Delta x} \left[ \alpha_{i+1/2} c_{i+1/2} (\mathbf{v}_{i+1/2}^+ - \mathbf{v}_{i+1/2}^-) - \alpha_{i-1/2} c_{i-1/2} (\mathbf{v}_{i-1/2}^+ - \mathbf{v}_{i-1/2}^-) \right] = \Delta t \mathbf{s}_i, \end{aligned} \quad (6.1)$$

where  $\mathbf{g}_{i+1/2}^L$  is the Rusanov numerical flux (2.2).

Then the discrete cell entropy inequality (1.10) can be written in the form

$$\begin{aligned} U(\hat{\mathbf{v}}_i) - U(\mathbf{v}_i) + \frac{\Delta t}{\Delta x} \left[ G_{i+1/2}^L(\mathbf{v}_{i+1/2}^-, \mathbf{v}_{i+1/2}^+) - G_{i-1/2}^L(\mathbf{v}_{i-1/2}^-, \mathbf{v}_{i+1/2}^+) \right] \\ + \alpha_{i+1/2} \frac{c_{i+1/2}}{2} (U(\mathbf{v}_{i+1/2}^+) - U(\mathbf{v}_{i+1/2}^-)) - \alpha_{i-1/2} \frac{c_{i-1/2}}{2} (U(\mathbf{v}_{i-1/2}^+) - U(\mathbf{v}_{i-1/2}^-)) \leq 0 \end{aligned} \quad (6.2)$$

with the proper numerical entropy flux (3.9).

Below we will mark the numerical solutions of scheme (6.1)-(6.2) with a label indicating how the flux limiters are calculated. The letters  $L$  and  $A$  denote the applying linear programming or approximate solution to the optimization problem, respectively. The letters  $H$ ,  $Q$  and  $E$  mean that the flux limiters were calculated using inequalities (4.14), (4.15) and (6.2), respectively. Numerical solutions with flux limiters satisfying inequalities (2.13) are denoted as  $PP$ . In the latter case, flux limiters are defined as follows

$$\alpha_{i+1/2} = \max \left( 0, \min \left( 1, 1 - \frac{u_{i+1}}{c_{i+1/2}}, 1 + \frac{u_i}{c_{i+1/2}} \right) \right). \quad (6.3)$$

In addition, we use the following labels:

HR1 is a first-order hydrostatic reconstruction scheme with HLL numerical flux given in [6];

HR2 is a hydrostatic reconstruction scheme of second-order spatial accuracy with explicit Euler time integration proposed in [5];

ZL is a characteristic variable implementation of the Boris-Book flux limiter described in [32] and applied to the HR scheme (2.1)-(2.2).

To solve linear programming problems we apply GLPK package v.4.65 (<https://www.gnu.org/software/glpk/>).

### 6.1 One-Dimensional Dam Break Over a Wet Flat Bed

In this section, we consider a dam break on a wet flat bed in a frictionless, horizontal, rectangular channel. The channel is 1000 m long. The dam is located in the middle of the channel. The water depth at the left and right hand sides of the dam is 100 m and 1 m, respectively. The



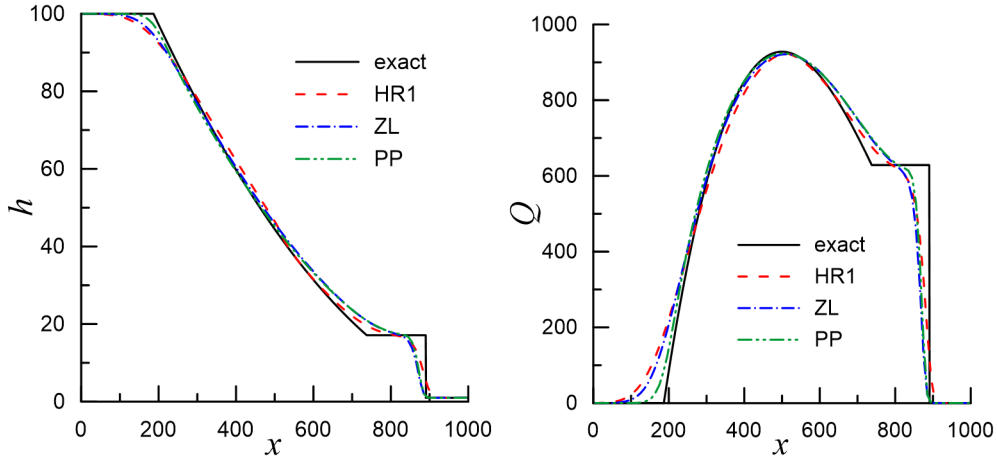


Figure 1: One-dimensional dam break over a wet flat bed. Comparisons of exact solutions with simulated water depths (left) and discharges (right) using HR1, ZL, and PP at  $t=10$  s. The number of cells is  $N=100$ .

dam instantly collapses across its entire width and the resulting flow consists of a shock wave traveling downstream and a rarefaction wave traveling upstream. In this problem there is a transition from subcritical upstream to supercritical downstream flows. The simulation is performed up to time  $t=10$  s.

The analytical solution of this problem was given by Stoker (1957) [28]. The 1D dam-break on a wet flat bed is a classical test to verify the shock-capturing ability of numerical schemes.

Numerical results obtained with different schemes at time  $t=10$  s on a uniform grid of  $N=100$  cells are shown in Fig. 1-Fig. 3. As shown in Fig. 2, the shock wave resolutions using HR2, LHE, and LHQE are less dissipative (sharper) and better than with the other schemes shown in Fig. 1.

The simulated results with PP are close to those obtained with ZL but require much less calculations. In the numerical results with LHE, AHE, LHQE, and AHQE, we observe the so-called "terracing" phenomenon characteristic of FCT methods. Numerical results for water discharge obtained using the LHE and AHE schemes have oscillations that are absent in the velocities (Fig 3).

The analytical and numerical solutions were compared quantitatively by the  $L^1$  error. The error is defined as

$$L^1 = \frac{1}{N} \sum_{i=1}^N |y_i - y^a(x_i)| \quad (6.4)$$

where  $y_i$  is the numerical and  $y^a$  is the analytical solution at point  $x_i$ ,  $N$  means the number of these points. Table 1 shows the  $L^1$ -norms of errors of the numerical solutions obtained with different schemes.

A comparison of analytical solutions with computed depths, as well as velocities and discharges at  $t=10$  s using LHE(LHQE) and AHE(AHQE) are given in Fig. 3. The flux limiters for LHE(LHQE) and AHE(AHQE) are calculated using exact and approximate solutions to linear programming problems. We note good agreement between these numerical solutions, and the addition of constraints on water discharges to calculate flux limiters leads to suppression of oscillations in the numerical solutions.

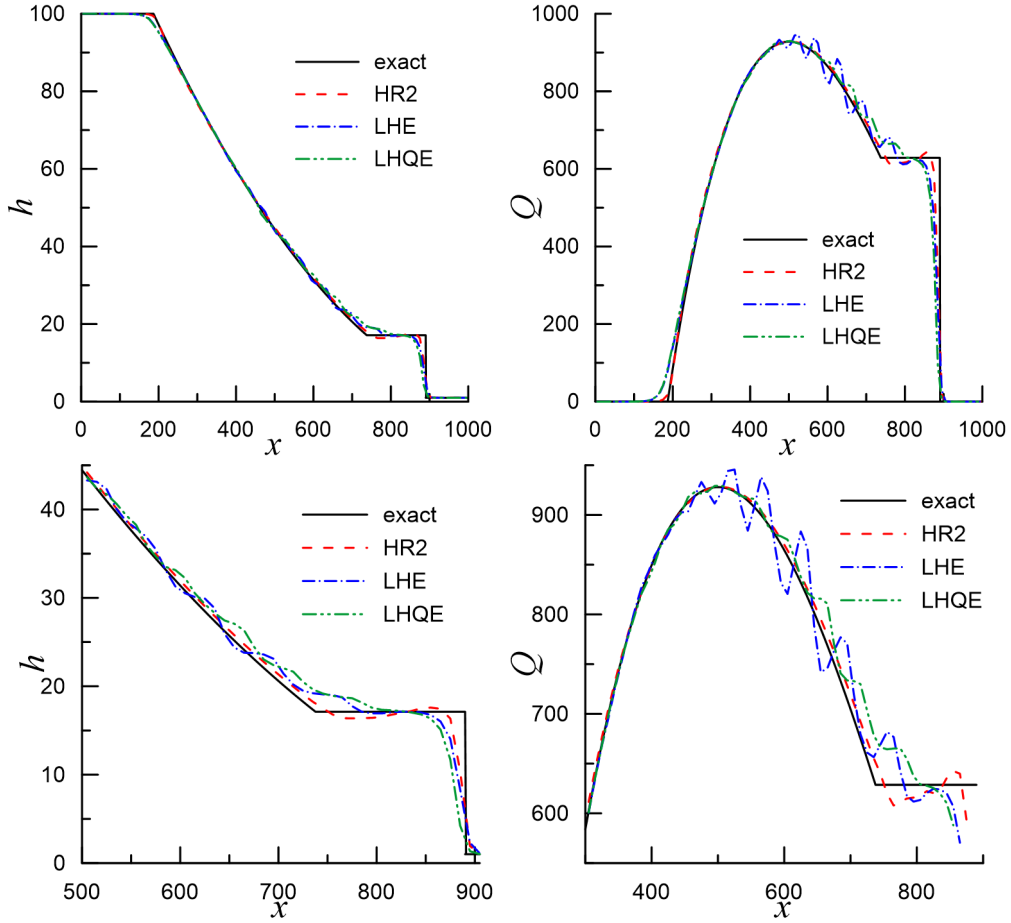


Figure 2: One-dimensional dam break over a wet flat bed. Comparisons of exact solutions with simulated water depths (left) and discharges (right) using HR2, LHE, and LHQE at  $t=10$  s. The second row is a zoom in the area behind the shock. The number of cells is  $N=100$ .

Table 1:  $L^1$ -norms of errors for the numerical solutions of the 1D dam break over a wet flat bed at  $t=10$  s with  $N=100$ .

	<i>HR1</i>	<i>ZL</i>	<i>PP</i>	<i>HR2</i>
H	$1.468 \times 10^0$	$1.679 \times 10^0$	$1.365 \times 10^0$	$4.052 \times 10^{-1}$
Q	$3.596 \times 10^1$	$3.882 \times 10^1$	$3.060 \times 10^1$	$9.180 \times 10^0$
	<i>LHE</i>	<i>AHE</i>	<i>LHQE</i>	<i>AHQE</i>
H	$6.153 \times 10^{-1}$	$5.114 \times 10^{-1}$	$7.898 \times 10^{-1}$	$6.306 \times 10^{-1}$
Q	$1.912 \times 10^1$	$1.619 \times 10^1$	$2.003 \times 10^1$	$1.647 \times 10^1$

## 6.2 One-Dimensional Dam Break Over a Dry Bed

The dry bed dam-break test is usually applied to verify the ability of a difference scheme to propagate a wet/dry front at the correct speed and to keep water depth positive. The analytical solution of this problem was given by Stoker (1957) [28].

We consider a rectangular channel with 1000 m length and a flat bed. The dam is located in the middle of the channel. The water depth at the left and right hand sides of the dam is 100 m and 0 m, respectively. The dam break is instantaneous and there is no friction. The

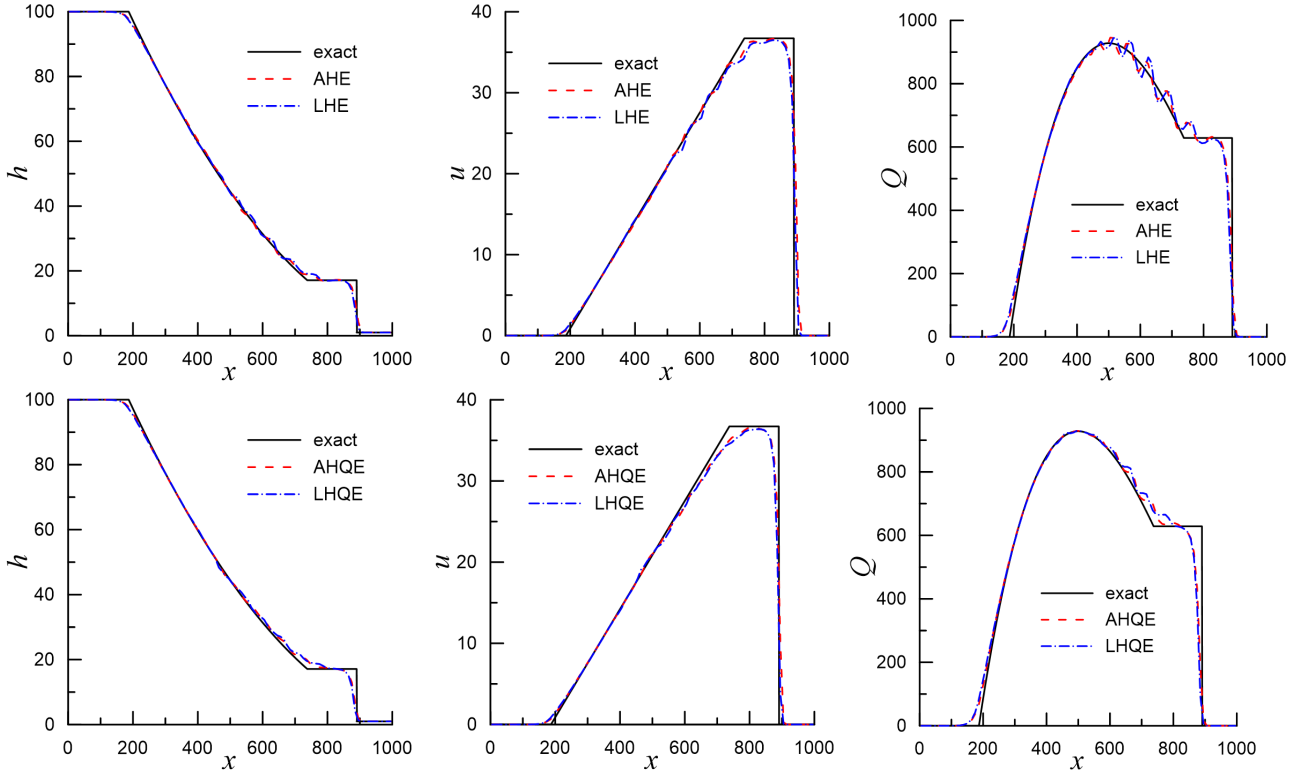


Figure 3: One-dimensional dam break over a wet flat bed. Comparisons of numerical results obtained with FCT schemes whose flux limiters are computed using exact and approximate solutions to a linear programming problem with discrete entropy inequality and different constraints. The number of cells is  $N=100$ .

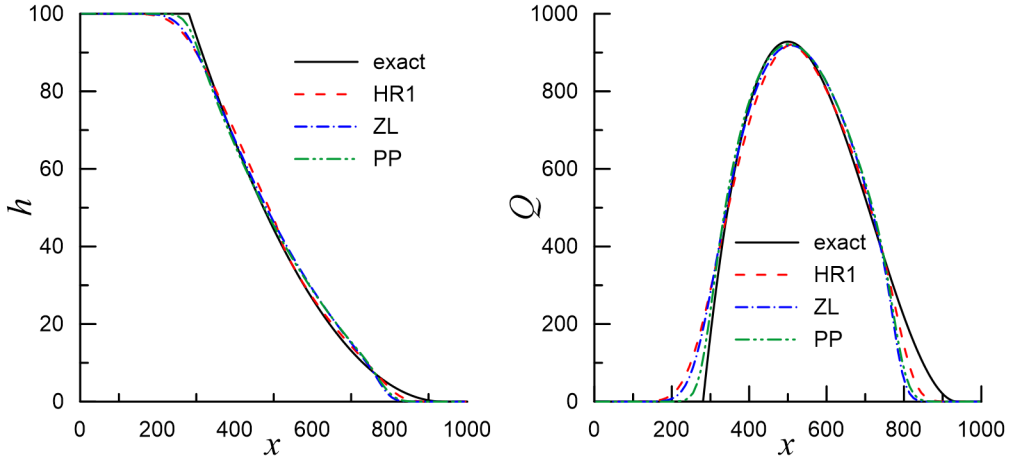


Figure 4: One-dimensional dam break over a dry bed. Comparisons of exact solutions with simulated water depths and discharges using HR1, ZL, and PP at time  $t=7$  s. The number of cells is  $N=100$ .

solution consists of a single rarefaction wave with a wet/dry front at its lower end.

The flow domain is discretized into 100 uniform cells. The simulation time is  $t=7$  s.

Comparisons of exact solutions with simulated depths as well as discharges at  $t=7$  s using the six schemes are presented in Fig. 4-5. Among the proposed schemes, the HR1, ZL, and

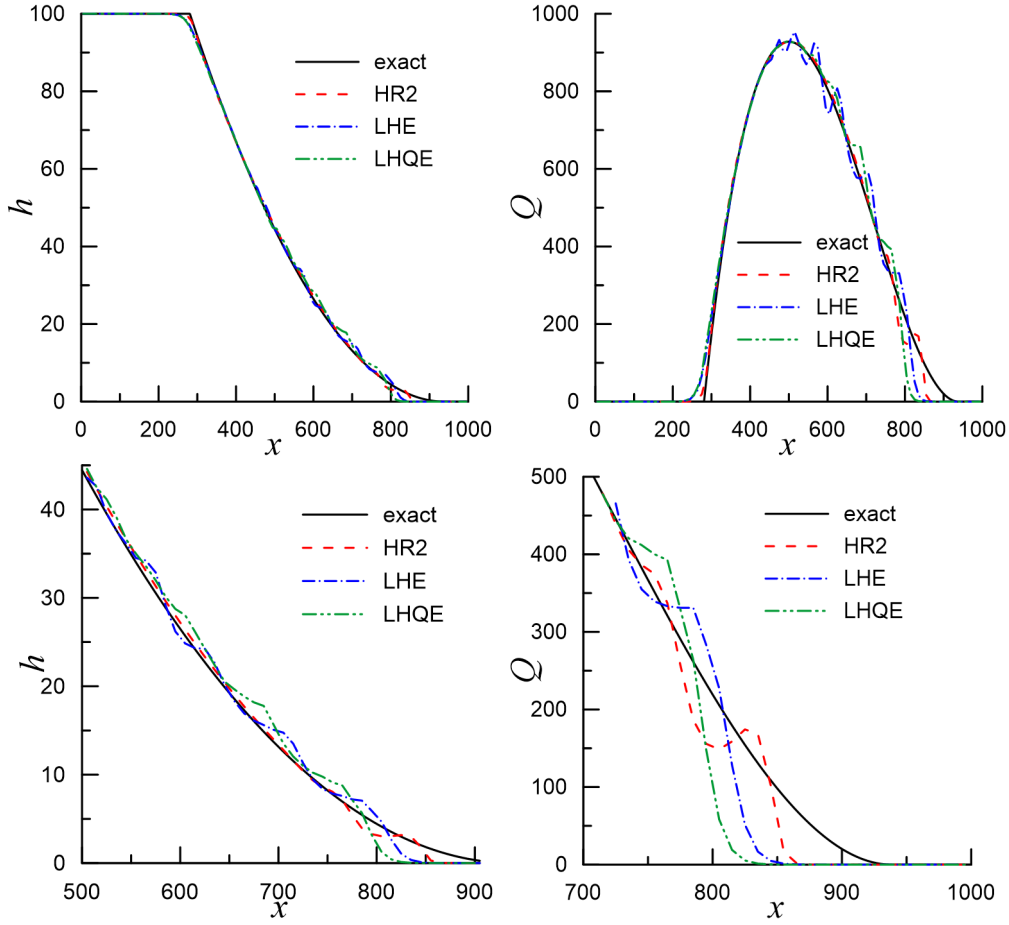


Figure 5: One-dimensional dam break over a dry bed. Comparisons of exact solutions with simulated water depths and discharges using HR2, LHE, and LHQE at time  $t=7$  s. The second row is a zoom in the area of the front of the moving water. The number of cells is  $N=100$ .

Table 2:  $L^1$ -norms of errors for the numerical solutions of the 1D dam break over a dry bed at  $t=7$  s with  $N=100$ .

	<i>HR1</i>	<i>ZL</i>	<i>PP</i>	<i>HR2</i>
H	$1.145 \times 10^0$	$1.320 \times 10^0$	$1.050 \times 10^0$	$3.684 \times 10^{-1}$
Q	$2.838 \times 10^1$	$3.218 \times 10^1$	$2.590 \times 10^1$	$1.038 \times 10^1$
	<i>LHE</i>	<i>AHE</i>	<i>LHQE</i>	<i>AHQE</i>
H	$5.463 \times 10^{-1}$	$5.216 \times 10^{-1}$	$7.690 \times 10^{-1}$	$5.786 \times 10^{-1}$
Q	$2.129 \times 10^1$	$1.978 \times 10^1$	$2.207 \times 10^1$	$1.820 \times 10^1$

PP schemes present more dissipative results than the HR2, LHE, and LHQE schemes. The simulated results with PP are close to those obtained with ZL but require much less calculations. In the numerical results obtained with LHE, AHE, LHQE, and AHQE, we observe the so-called "terracing" phenomenon, which is characteristic of FCT methods. The LHE and AHE schemes produce oscillations in the water discharges that are absent in the velocities (Fig 6). For all the considered schemes, the largest error is observed at the front of the moving water.

Adding constraints on water discharges to the LHQE scheme to calculate flux limiters eliminates oscillations in numerical solutions. The numerical results obtained with LHE(LHQE)

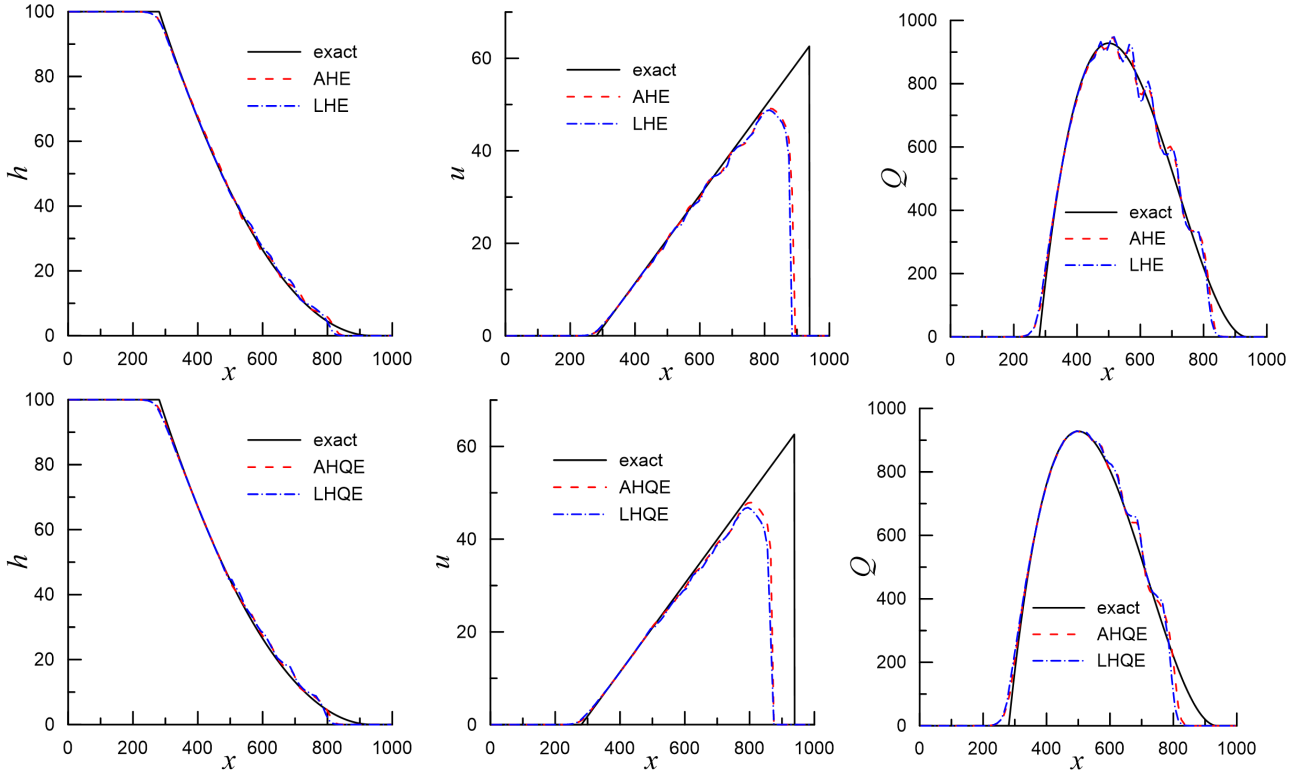


Figure 6: One-dimensional dam break over a dry bed. Comparisons of numerical results obtained with FCT schemes whose flux limiters are computed using exact and approximate solutions to a linear programming problem with discrete entropy inequality and different constraints at time  $t=7$  s.

and AHE(AHQE) are in a good agreement (Fig. 6). The flux limiters for LHE(LHQE) and AHE(AHQE) are calculated using exact and approximate solutions to linear programming problems.

### 6.3 Dam Break Over a Step.

In this test [5], a dam break over a downward bottom step is considered. The bottom topography and the initial data are given as follows

$$z(x) = \begin{cases} 1 & \text{if } x \leq 0, \\ 0 & \text{otherwise,} \end{cases} \quad h(x, 0) = \begin{cases} 0.75 & \text{if } x \leq 0, \\ 1.0 & \text{otherwise,} \end{cases} \quad Q(x, 0) = 0, \quad (6.5)$$

After a dam break, the solution consists of a left rarefaction wave, a stationary shock wave at an intermediate height of the bottom step between two stationary contact waves located at the bottom discontinuity, and a right shock wave [11, 22].

Comparisons of the numerical results obtained on a uniform grid of 200 cells with a reference solution at  $t=0.1$  after the dam break are shown in Fig. 7-9. The reference solution was calculated using a central-upwind scheme of second-order spatial accuracy [14] on a uniform grid with 2000 cells. In Fig. 7, the PP scheme generates oscillations in the numerical results in the area of the bottom discontinuity. In the numerical results obtained with the ZL scheme, we see an overshoot of the water depth and discharge for the right shock wave. The second-order HR2 scheme does not reproduce the left rarefaction wave in its whole entirety, as well

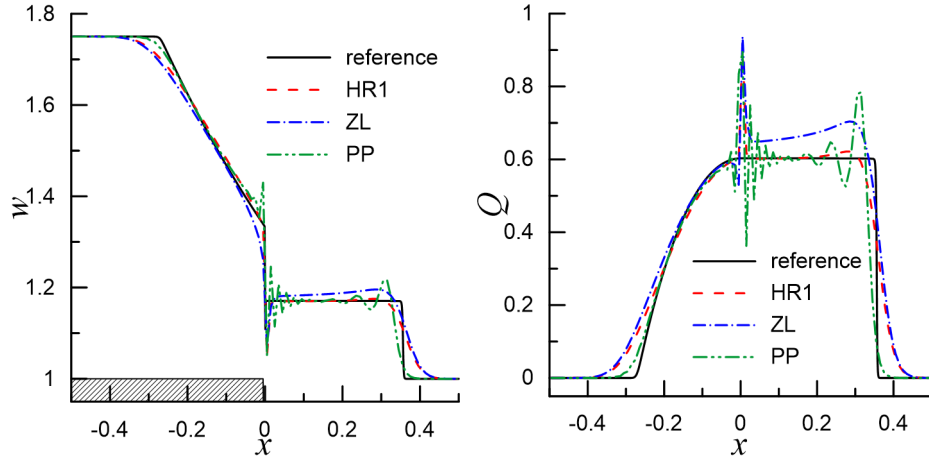


Figure 7: Dam break over a step. Comparisons of reference solutions with simulated water depths and discharges using the HR1, ZL, and PP schemes at time  $t=0.1$  s with  $N=200$  cells.

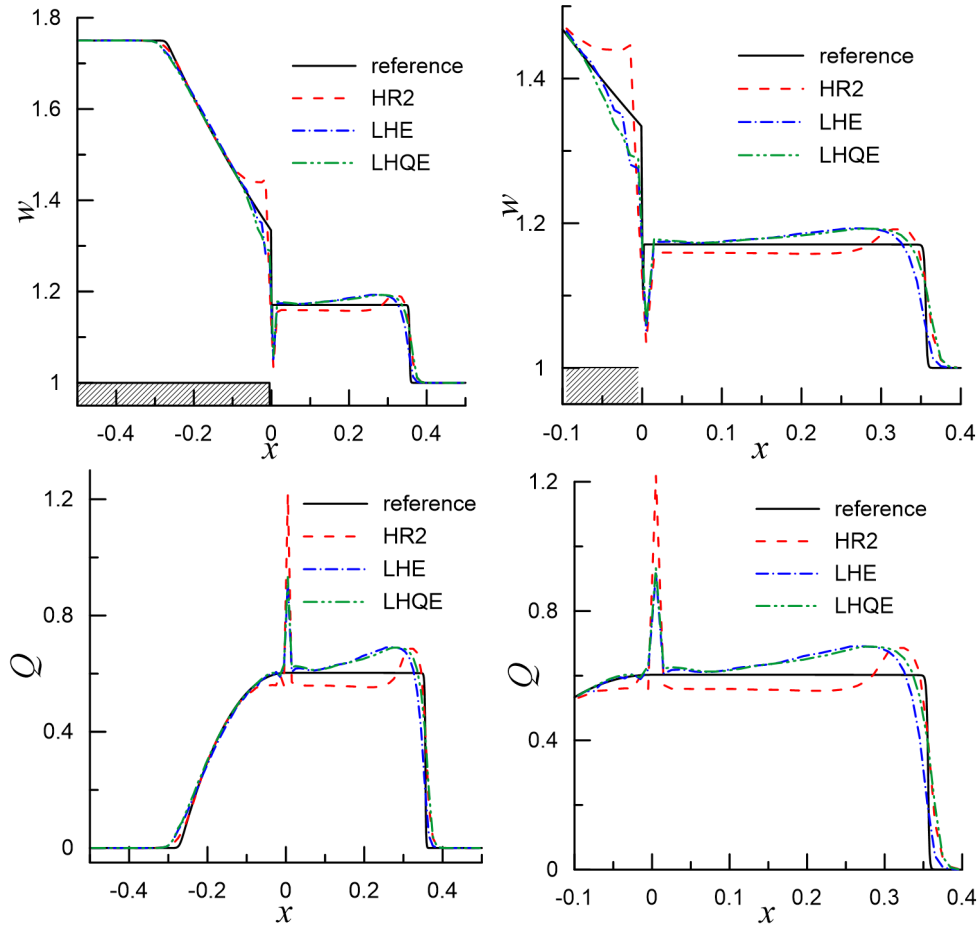


Figure 8: Dam break over a step. Comparisons of reference solutions with simulated water depths and discharges using HR2, LHE, and LHQE at time  $t=0.1$  s with  $N=200$  cells. On the right is a zoom of the area of the bottom discontinuity and the right shock wave.

as the shock wave (Fig. 8). In Fig. 8-9, the right side of the shock wave for the LHE, LHQE, AHE, and AHQE schemes shows an overshoot of the simulated water depth and discharge.

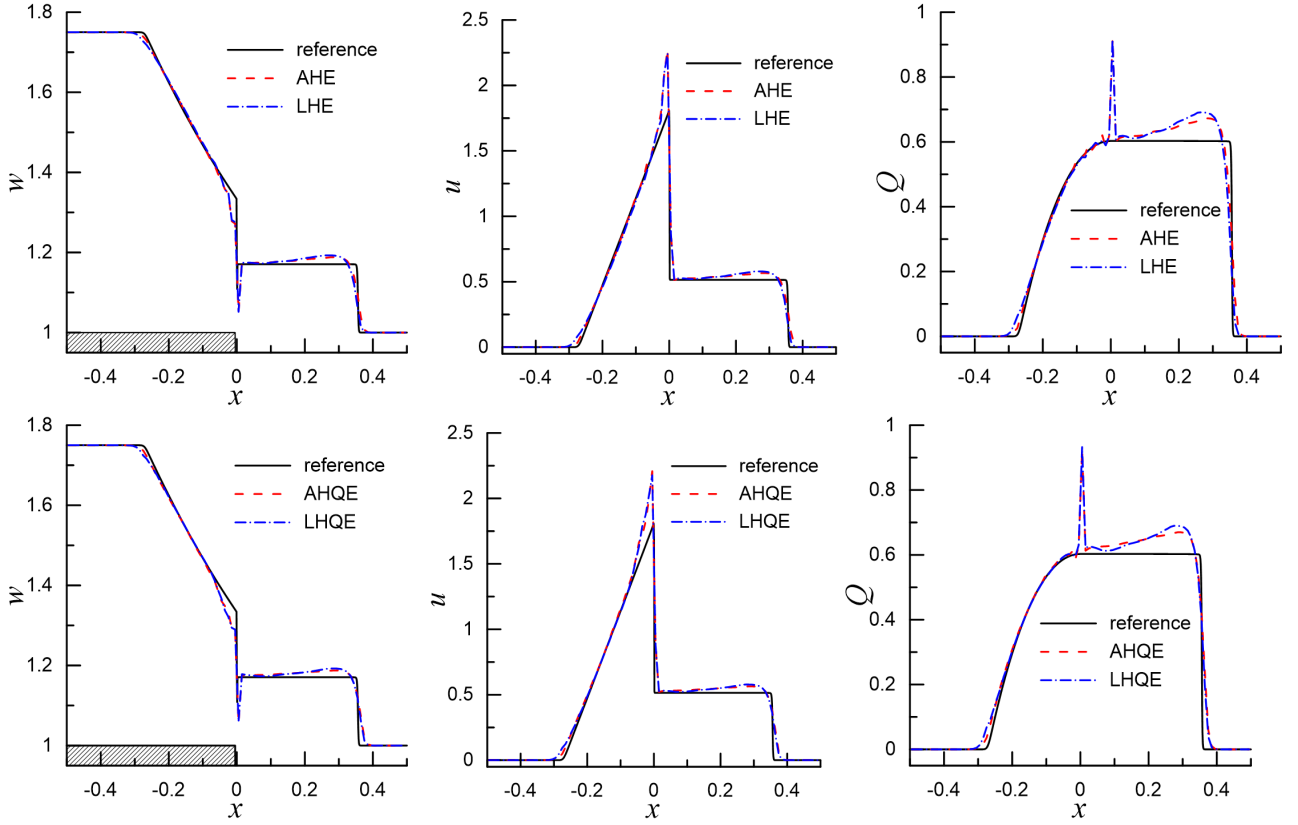


Figure 9: Dam break over a step. Comparisons of numerical results obtained with FCT schemes whose flux limiters are computed using exact and approximate solutions to a linear programming problem with discrete entropy inequality and different constraints. ( $t=0.1$  s,  $N=200$ ).

We note that none of the considered schemes reproduces the exact solution, especially in the bottom discontinuity. Table 3 shows the  $L^1$ -norm error between the reference solution and the numerical solutions at time  $t = 0.1$  for different difference schemes.

Table 3:  $L^1$ -norms of errors for the numerical solutions of the 1D dam break over a step at  $t = 0.1$  s with  $N=200$ .

	<i>HR1</i>	<i>ZL</i>	<i>PP</i>	<i>HR2</i>
H	$5.219 \times 10^{-3}$	$8.647 \times 10^{-3}$	$6.039 \times 10^{-3}$	$6.840 \times 10^{-3}$
Q	$1.390 \times 10^{-2}$	$2.489 \times 10^{-2}$	$1.806 \times 10^{-2}$	$1.703 \times 10^{-2}$
	<i>LHE</i>	<i>AHE</i>	<i>LHQE</i>	<i>AHQE</i>
H	$4.830 \times 10^{-3}$	$4.100 \times 10^{-3}$	$4.695 \times 10^{-3}$	$4.656 \times 10^{-3}$
Q	$1.326 \times 10^{-2}$	$1.096 \times 10^{-2}$	$1.243 \times 10^{-2}$	$1.209 \times 10^{-2}$

We also note that the numerical results obtained with LHE(LHQE) and AHE(AHQE) agree well (Fig. 9). The flux limiters for LHE(LHQE) and AHE(AHQE) are calculated using exact and approximate solutions to linear programming problems.

## 6.4 Steady Transcritical Flow With a Shock Over a Bump.

We consider a test taken from [9] consisting of a transcritical flow with a shock over a bump. The bed topography of a rectangular channel 25 m long is given as follows

$$z(x) = \begin{cases} 0.2 - 0.05(x - 10)^2 & \text{if } 8 < x < 12, \\ 0 & \text{otherwise.} \end{cases} \quad (6.6)$$

Initial conditions satisfy the hydrostatic equilibrium

$$h + z = 0.33 \quad \text{and} \quad Q = 0. \quad (6.7)$$

Discharge  $Q = 0.18 \text{ m}^2/\text{s}$  and water level  $h + z = 0.33 \text{ m}$  were set as upstream and downstream boundary conditions. In the steady-state solution, the flow to the left of the bump is subcritical, then closer to the end of the bump it becomes supercritical, and after a hydraulic jump it is subcritical again.

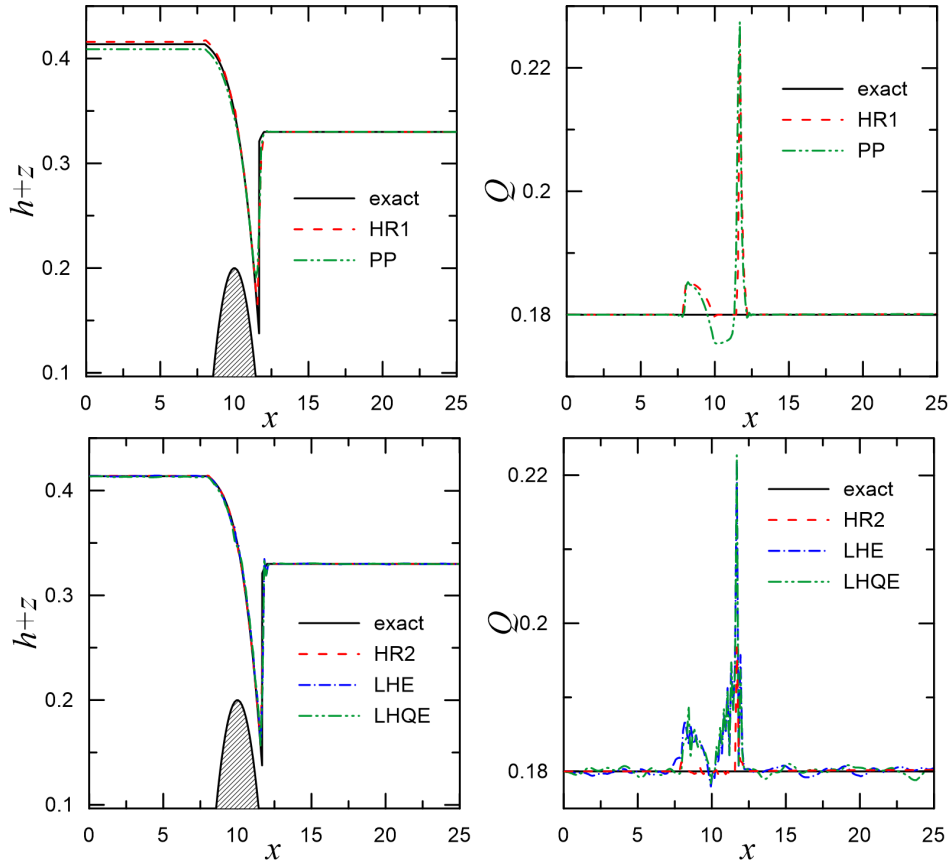


Figure 10: Steady transcritical flow with a shock over a bump. Comparison of exact solutions with computed water depths and discharges obtained by HR1, PP, HR2, LHE, and LHQE with  $N=100$ .

Numerical results for the steady state, obtained on a uniform grid of 100 cells, are shown in Fig. 10-11. In the numerical results obtained with the HR1 scheme, we observe an overshoot of the free surface before the bump and an undershoot of the free surface for the PP scheme. The free water surfaces calculated with HR2, LHE, and LHQE agree fairly well with the analytical



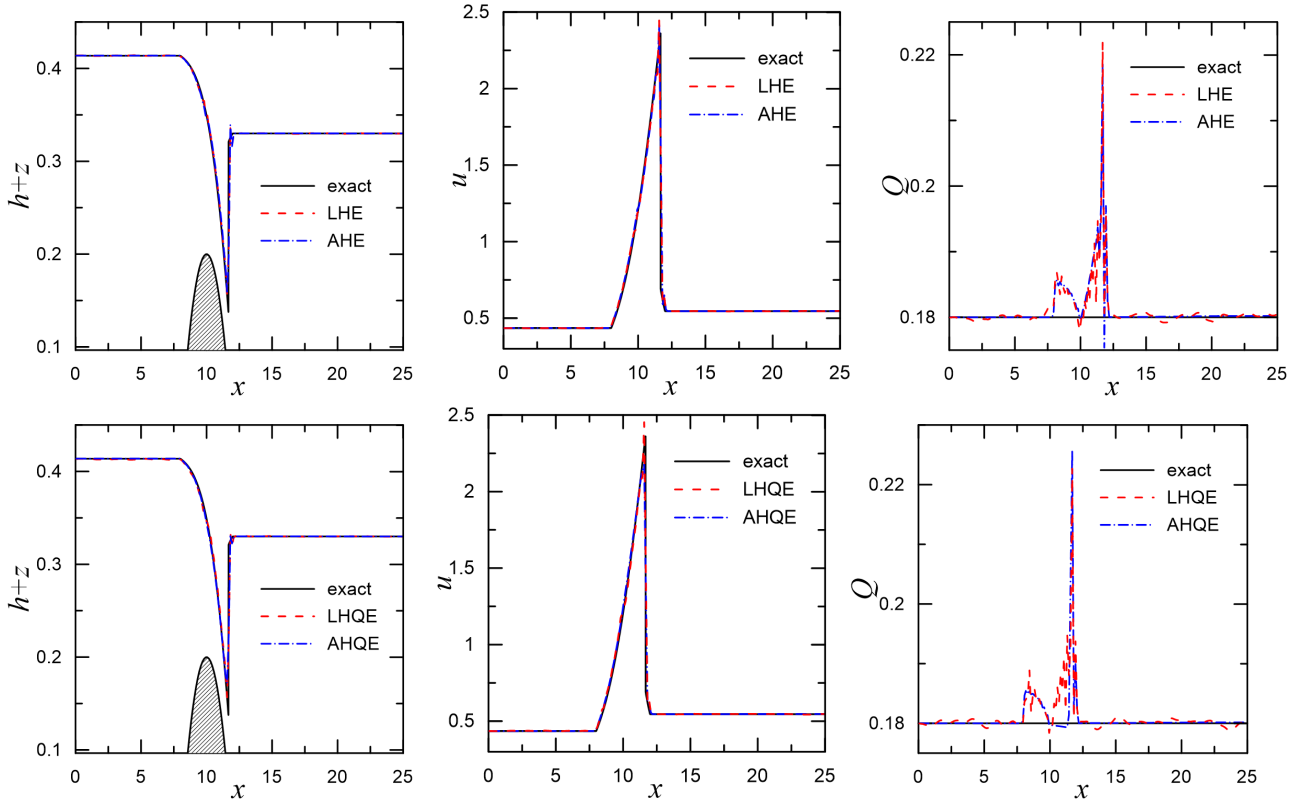


Figure 11: Steady transcritical flow with a shock over a bump. Comparisons of numerical results obtained with FCT schemes whose flux limiters are computed using exact and approximate solutions to a linear programming problem with discrete entropy inequality and different constraints.

Table 4:  $L^1$ -norms of errors of the transcritical steady state flow with a shock over a bump.

	<i>HR1</i>	<i>PP</i>	<i>HR2</i>	
H	$1.633 \times 10^{-3}$	$2.858 \times 10^{-3}$	$6.258 \times 10^{-4}$	
Q	$7.534 \times 10^{-4}$	$1.106 \times 10^{-3}$	$2.201 \times 10^{-4}$	
	<i>LHE</i>	<i>AHE</i>	<i>LHQE</i>	<i>AHQE</i>
H	$1.298 \times 10^{-3}$	$1.298 \times 10^{-3}$	$1.501 \times 10^{-3}$	$9.556 \times 10^{-4}$
Q	$1.270 \times 10^{-3}$	$1.087 \times 10^{-3}$	$1.282 \times 10^{-3}$	$8.034 \times 10^{-4}$

solution, with slight deviations around the hydraulic jump. Numerical oscillations for water discharges near the hydraulic jump are present for all compared schemes. Small oscillations are also present in the calculated discharges with the LHE and LHQE schemes in the whole modeling area. The  $L^1$ -norm error between the exact and numerical solutions are shown in Table 4.

Note that none of the considered schemes is well-balanced for moving water steady states with non-zero discharges.

We also note that the numerical results obtained with LHE(LHQE) and AHE(AHQE) agree well (Fig. 11). The flux limiters for LHE(LHQE) and AHE(AHQE) are calculated using exact and approximate solutions to linear programming problems.

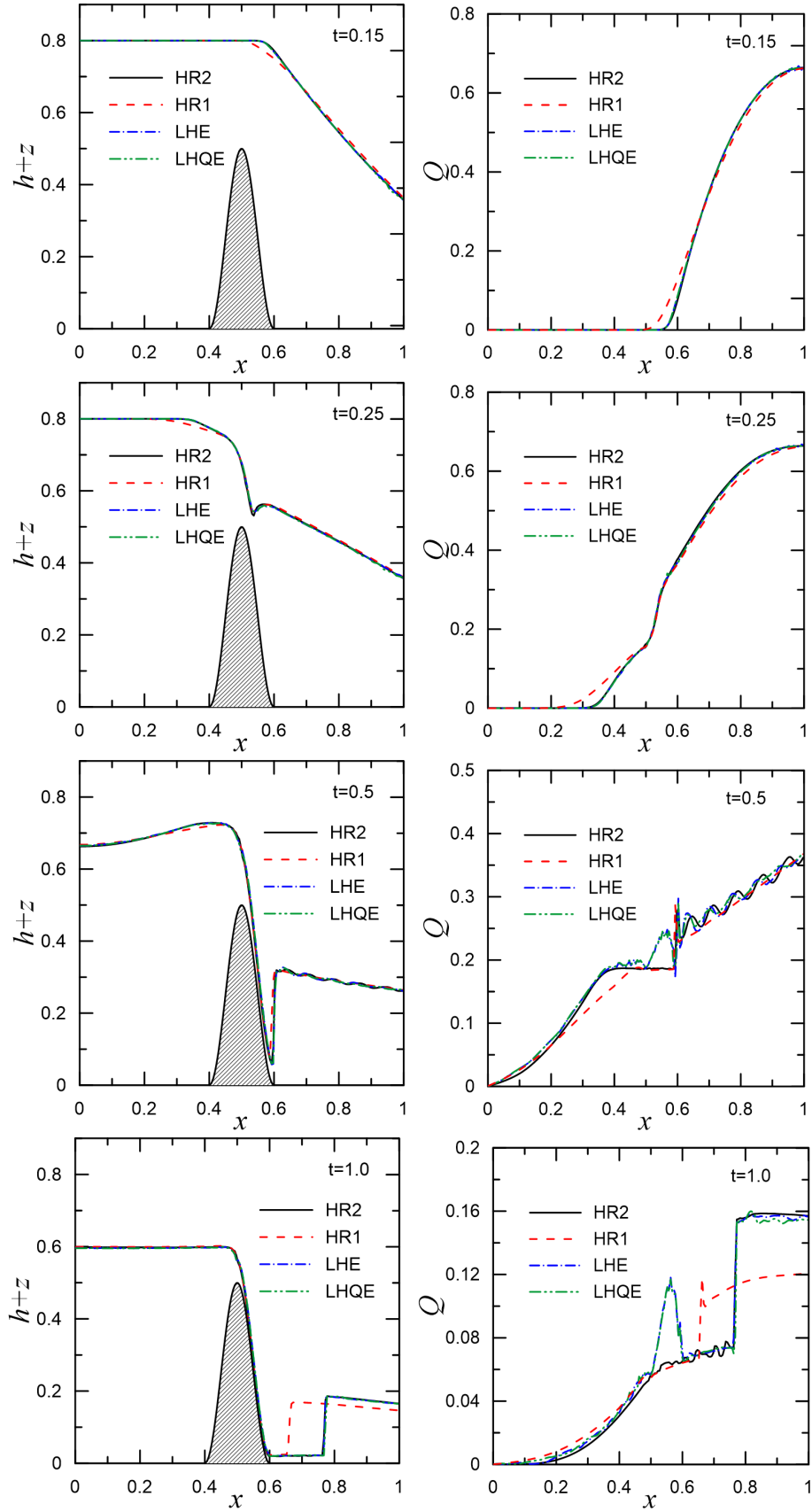


Figure 12: Drainage on a non-flat bottom. Water levels and discharges at various times  $t=0.15, 0.25, 0.5, 1.0$  s.

## 6.5 Drainage on a Non-Flat Bottom

We consider drainage of a symmetric rectangular reservoir to a dry bed through its boundaries, leaving water in topographic depressions. Due to the symmetry, the flow is computed on half the domain, with wall boundary conditions on the left boundary, and open boundary conditions on the right boundary. The boundary condition on the right side of the domain allows water that was at rest to flow freely through the right boundary into the originally dry region. The bottom topography consists of one hump

$$z(x) = \begin{cases} 0.25 [1 + \cos(\pi(x - 0.5)/0.1)] & \text{if } |x - 0.5| < 0.1, \\ 0 & \text{otherwise .} \end{cases} \quad (6.8)$$

After drainage begins, the solution converges to a steady-state solution in which water exists only to the left of the hump.

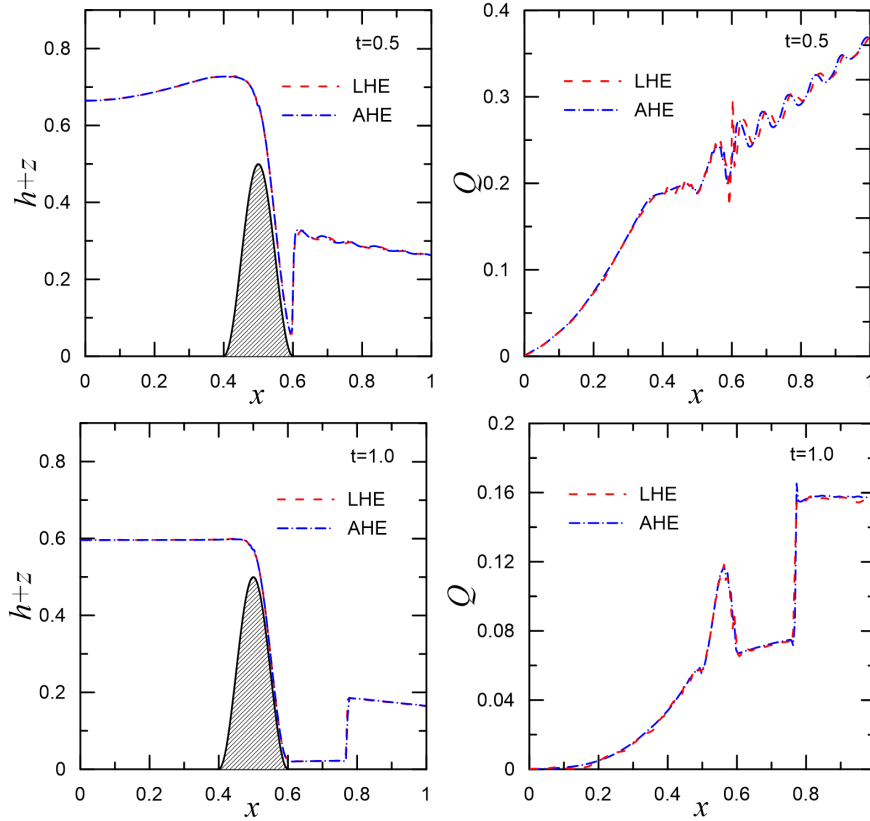


Figure 13: Drainage on a non-flat bottom. Water levels and discharges at times  $t=0.5, 1.0$  s.

Numerical results of water flow at different times, obtained on a uniform grid with  $N=200$  cells, are presented in Fig. 12-14. Fig. 12 shows that all numerical schemes, except HR1, give similar results for the water surface level. The first-order HR1 scheme produces a more diffusive water level profile. The most significant difference in the computed discharges is observed over the right side of the hump.

In Fig. 13, the numerical results obtained with the LHE and AHE schemes are in good agreement, in contrast to the results presented in Fig. 14.

Note that the AHE and AHQE schemes use flux limiters, which are approximate solutions of the corresponding linear programming problems. The numerical results in Fig. 14 show their strong dependence on the numerical diffusion of the applied difference schemes.

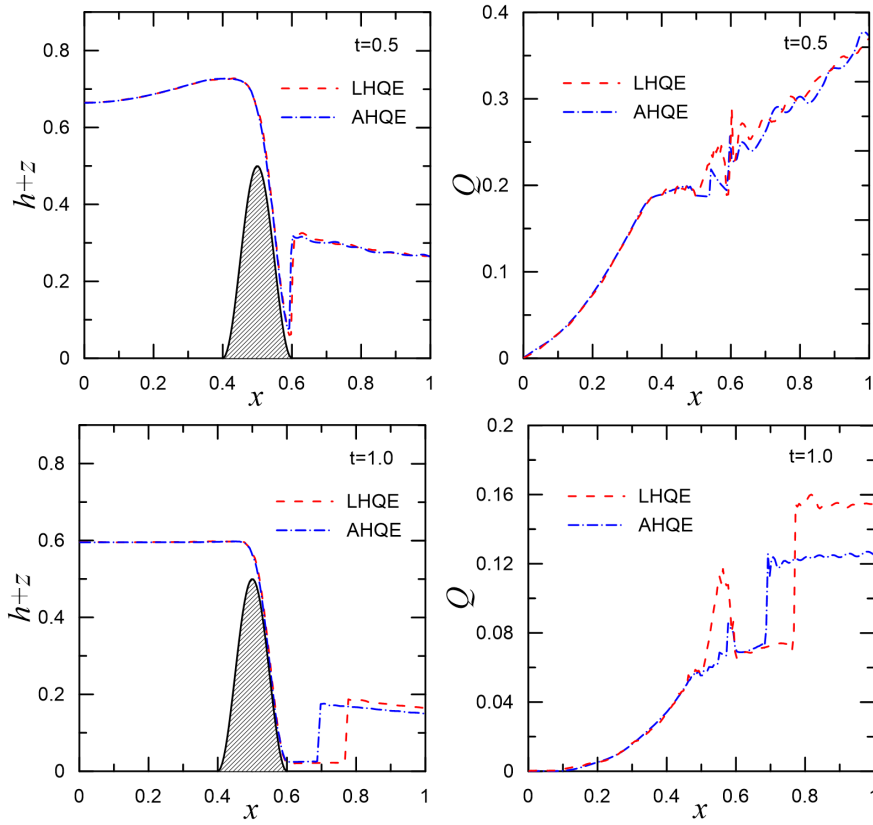


Figure 14: Drainage on a non-flat bottom. Water levels and discharges at times  $t=0.5, 1.0$  s.

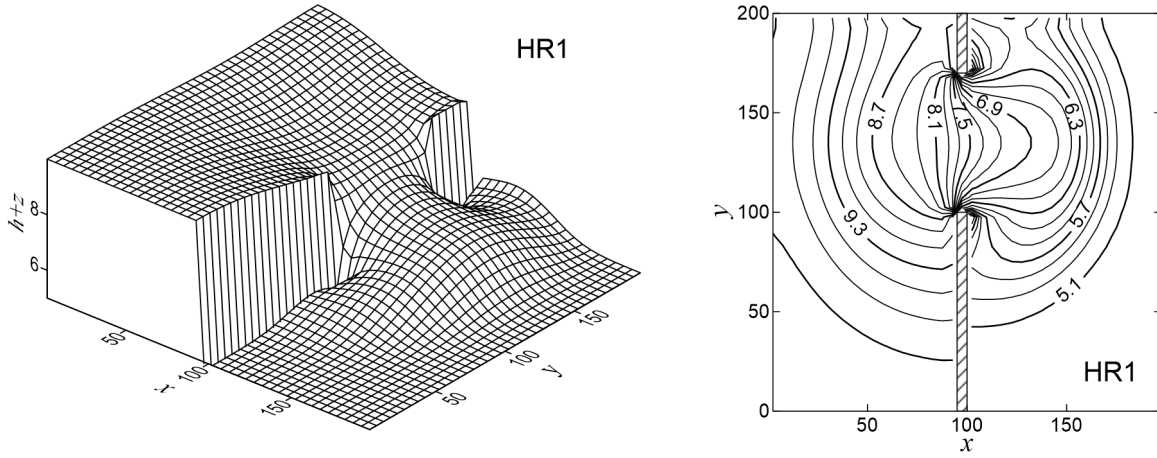


Figure 15: Water surface levels and depth contours for the partial dam-break flow at  $t = 7.2$  s computed with the HR1 scheme.

## 6.6 2D Partial Dam Break

In this section, a partial dam break problem with a nonsymmetrical breach is considered. The spatial domain is defined as a channel with 200 m in length and 200 m in width, the dam is located in the middle of the domain at a distance of 100 m. The bottom is horizontal and frictionless. Initially, the upstream and downstream water depths are set at 10 and 5 m, respectively. The breach is 75 m long, located 30 m from the left bank and 95 m from the right

bank.

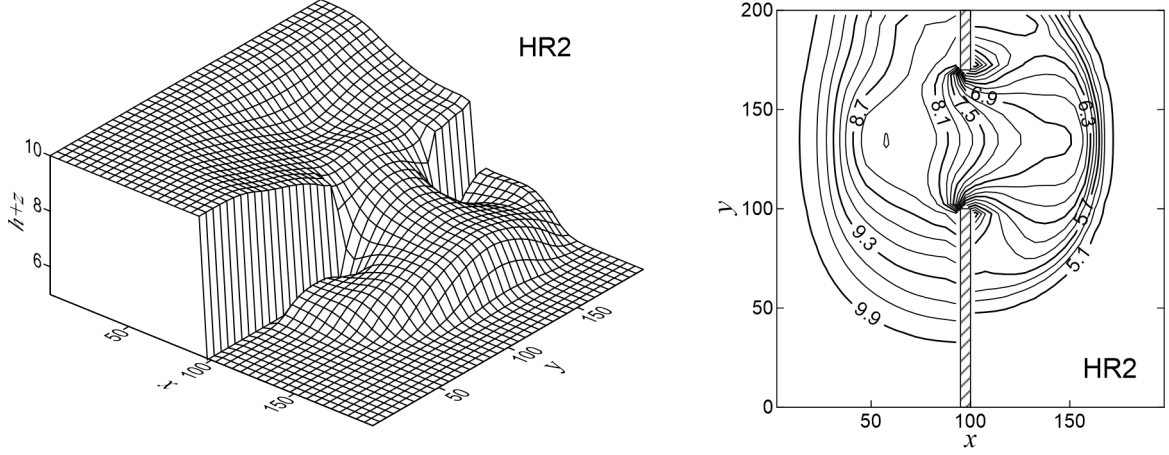


Figure 16: Water surface levels and depth contours for the partial dam-break flow at  $t = 7.2$  s computed with the HR2 scheme.

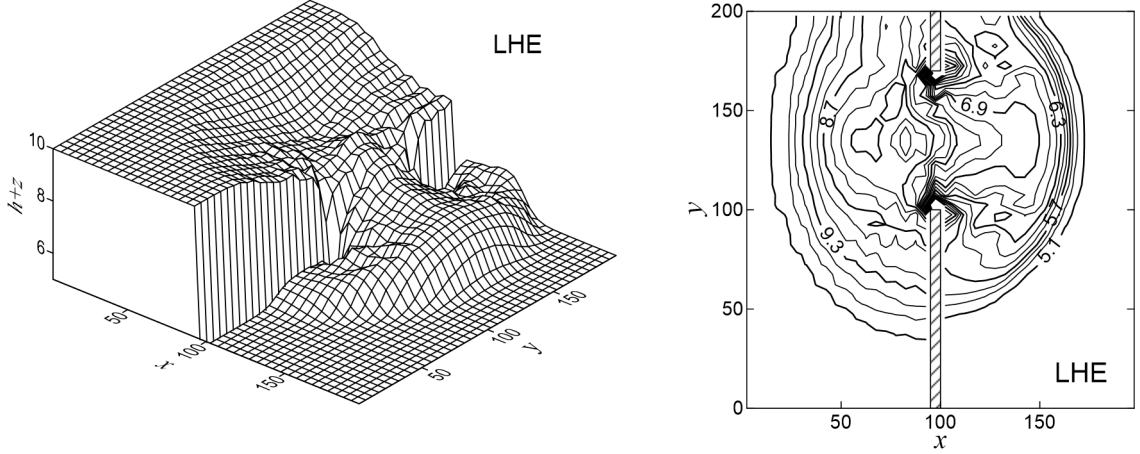


Figure 17: Water surface levels and depth contours for the partial dam-break flow at  $t = 7.2$  s computed with the LHE scheme.

The computational domain is discretized by a  $40 \times 40$  square grid. Fig. 15-20 show a three-dimensional view of the water surface levels and water depth contours 7.2 s after the dam failure. The numerical results obtained with the HR1 scheme are the most diffusive of the others. The water surface levels and water depth countours obtained by the LHE, LHQE, AHE, and AHQE schemes are similar to the numerical results of HR2 but are non-smooth. AHE and AHQE, whose flux limiters are approximate solutions to the corresponding optimization problems, produce smoother solutions than LHE and LHQE, but their solutions are nonsymmetric about the center of the breach.

## 7 Conclusions

We presented the flux correction design for a hybrid scheme to obtain an entropy-stable solution of shallow water equations with variable topography. The hybrid scheme is an explicit HR

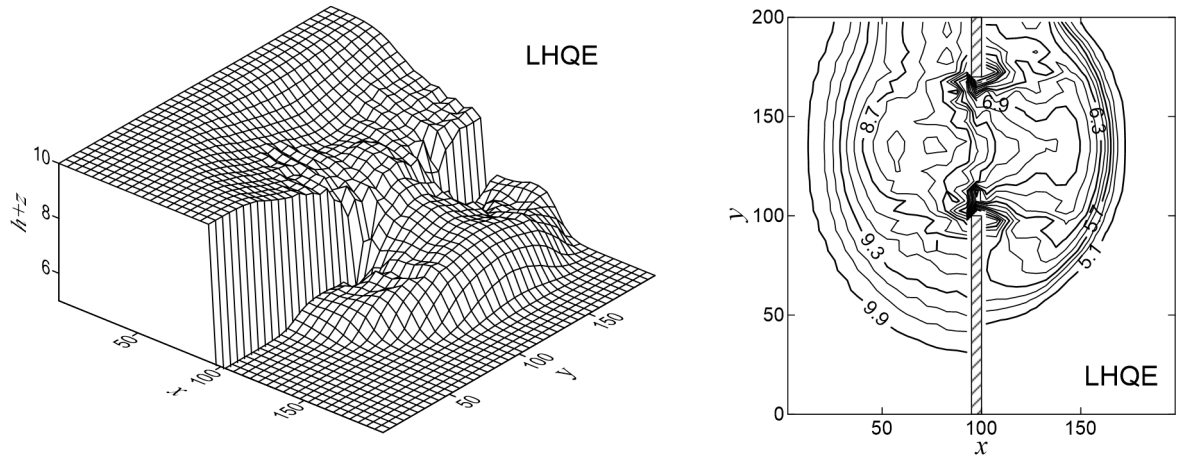


Figure 18: Water surface levels and depth contours for the partial dam-break flow at  $t = 7.2$  s computed with the LHQE scheme.

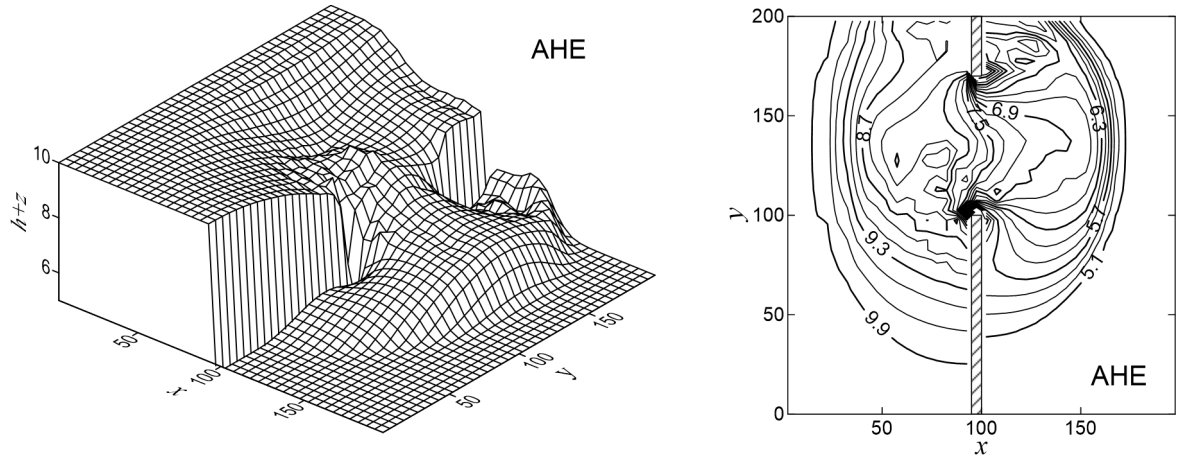


Figure 19: Water surface levels and depth contours for the partial dam-break flow at  $t = 7.2$  s computed with the AHE scheme.

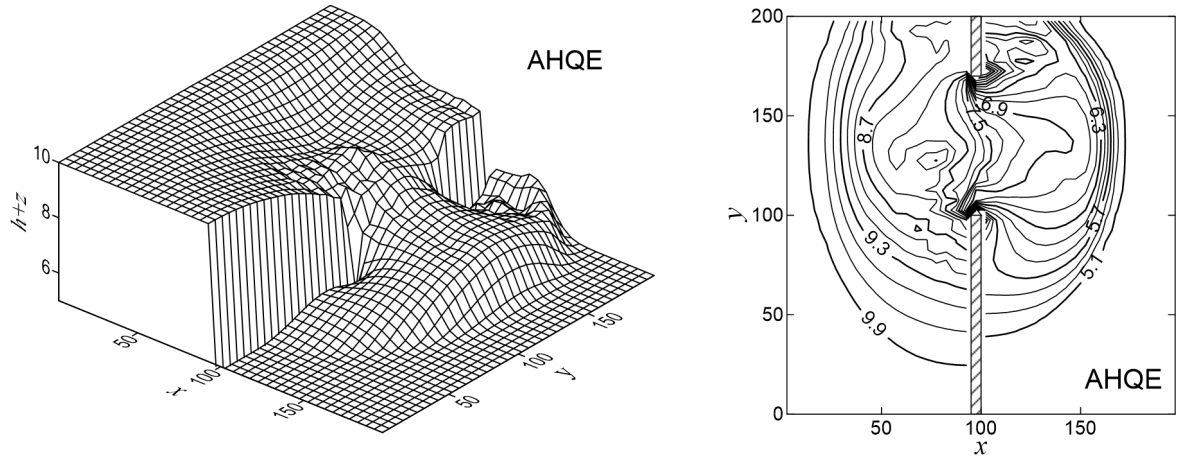


Figure 20: Water surface levels and depth contours for the partial dam-break flow at  $t = 7.2$  s computed with the AHQE scheme.

scheme whose numerical flux is a convex combination of a first-order Rusanov flux and a high-order flux. We studied the conditions under which a first-order HR scheme with the Rusanov flux satisfied the fully discrete entropy inequality. The flux limiters for the hybrid scheme can be an exact or approximate solution to the corresponding optimization problem in which constraints valid for the first-order HR scheme are applied to the hybrid scheme. It is proved that in the vicinity of a numerical solution of the first-order HR scheme, there is a unique flux correction with flux limiters that are the proposed approximate solution to the optimization problem.

Numerical examples show that the hybrid HR scheme can produce oscillations in numerical results if only water surface level constraints for the optimization problem are used to compute the flux limiters. We also note that numerical results obtained with hybrid HR schemes whose flux limiters are exact and approximate solutions to the optimization problem can differ significantly.

## Conflict of interest

The author declare that he has no conflict of interest.

## Data Availability Statement

All data generated or analysed during this study are included in this published article.

## References

- [1] Audusse, E., Bouchut, F., Bristeau, M.-O., Klein, R., and Perthame, B.: A fast and stable well-balanced scheme with hydrostatic reconstruction for shallow water flows. *SIAM Journal on Scientific Computing*, 25(6),2050-2065 (2004). <https://doi.org/10.1137/S1064827503431090>
- [2] Audusse, E., Bouchut, F., Bristeau, M.-O., Sainte-Marie, J.: Kinetic entropy inequality and hydrostatic reconstruction scheme for the Saint-Venant system. *Math. Comput.* 85(302), 2815–2837 (2016). <https://doi.org/10.1090/mcom/3099>.
- [3] Berthon, C., Duran, A., Foucher, F., Saleh, K., de Dieu Zabsonré J.: Improvement of the hydrostatic reconstruction scheme to get fully discrete entropy inequalities. *J Sci Comput* 80, 924–956 (2019). <https://doi.org/10.1007/s10915-019-00961-y>
- [4] Boris, J.P., Book,D.L.: Flux-corrected transport. I. SHASTA, A fluid transport algorithm that works. *J. Comput. Phys.* **11**(1), 38-69 (1973). [https://dx.doi.org/10.1016/0021-9991\(73\)90147-2](https://dx.doi.org/10.1016/0021-9991(73)90147-2)
- [5] Buttinger-Kreuzhuber, A., Horváth, Z., Noelle, S., Blöschl, G., Waser, J.: A fast second-order shallow water scheme on two-dimensional structured grids over abrupt topography. *Advances in Water Resources*, 127,89-108 (2019). <https://doi.org/10.1016/j.advwatres.2019.03.010>
- [6] Chen, G., Noelle, S.: A new hydrostatic reconstruction scheme based on sub-cell reconstructions. *SIAM Journal on Numerical Analysis*, 55(2),758-784 (2017). <https://doi.org/10.1137/15M1053074>

- [7] Chen, T., Shu, C.-W.: Entropy stable high order discontinuous Galerkin methods with suitable quadrature rules for hyperbolic conservation laws. *Journal of Computational Physics* 345, 427–461 (2017). <https://doi.org/10.1016/j.jcp.2017.05.025>
- [8] Delestre, O., Cordier, S., Darboux, F., James, F.: A limitation of the hydrostatic reconstruction technique for Shallow Water equations. *Comptes Rendus Mathematique*, 350(13-14), 677–681 (2012). doi:10.1016/j.crma.2012.08.004
- [9] Delestre, O., Lucas, C., Ksinant, P.-A., Darboux, F., Laguerre, C., Vo, T.-N.-T., James, F., Cordier, S.: SWASHES: a compilation of shallow water analytic solutions for hydraulic and environmental studies. *International Journal for Numerical Methods in Fluids*, 72(3), 269–300 (2013). <https://doi.org/10.1002/fld.3741>.
- [10] Fjordholm, U., Mishra, S., Tadmor, E.: Arbitrarily high-order accurate entropy stable essentially nonoscillatory schemes for systems of conservation laws. *SIAM J. Numer. Anal.* 50(2), 544–573 (2012). <https://doi.org/10.1137/110836961>
- [11] Han, E., Warnecke, G.: Exact Riemann solutions to shallow water equations. *Quart. Appl. Math.* 72 (3), 407–453 (2014). <https://doi.org/10.1090/S0033-569X-2014-01353-3>.
- [12] Harten, A., Hyman, J.M., Lax, P.D., Keyfitz, B.: On finite-difference approximations and entropy conditions for shocks. *Comm. Pure Appl. Math.* 29(3), 297–322 (1976). <https://doi.org/10.1002/cpa.3160290305>
- [13] Hildebrand, A., Mishra, S.: Entropy stable shock capturing space-time discontinuous Galerkin schemes for systems of conservation laws. *Numer. Math.* 126(1), 103–151 (2014). <https://doi.org/10.1007/s00211-013-0558-0>
- [14] Kivva, S., Zheleznyak, M., Pylypenko, O., Yoschenko, V.: Open Water Flow in a Wet/Dry Multiply-Connected Channel Network: A Robust Numerical Modeling Algorithm. *Pure Appl. Geophys.* 177, 3421–3458 (2020). <https://doi.org/10.1007/s00024-020-02416-0>.
- [15] Kivva, S.: Flux-corrected transport for scalar hyperbolic conservation laws and convection-diffusion equations by using linear programming. *J Comput Phys* 425, 109874 (2021). <https://doi.org/10.1016/j.jcp.2020.109874>
- [16] Kivva, S.: Entropy Stable Flux Correction for Scalar Hyperbolic Conservation Laws. *J Sci Comput* 91, 10 (2022). <https://doi.org/10.1007/s10915-022-01792-0>
- [17] Kuzmin, D.: Explicit and implicit FEM-FCT algorithms with flux linearization. *J. Comput. Phys.* 228(7), 2517–2534 (2009). <https://dx.doi.org/10.1016/j.jcp.2008.12.011>
- [18] Kuzmin, D., Moller, M., Turek, S.: High-resolution FEM-FCT schemes for multidimensional conservation laws. *Computer Meth. Appl. Mech. Engrg.* 193(45-47), 4915–4946 (2004). <https://dx.doi.org/10.1016/j.cma.2004.05.009>
- [19] Lax, P.: Hyperbolic Systems of Conservation Laws and Mathematical Theory of Shock Waves. In : Vol.11 of SIAM Regional Conference Series in Applied Mathematics. (1972)
- [20] Lefloch, P., Mercier, J.-M., Rohde, C.: Fully discrete, entropy conservative schemes of arbitrary order. *SIAM Journal on Numerical Analysis*, 40(5), 1968–1992 (2002) <https://doi.org/10.1137/S003614290240069X>



- [21] Merriam, M. L.: An entropy-based approach to nonlinear stability. NASA-TM-101086, Ames Research Center, Moffett Field, California (1989)
- [22] Minatti, L., Faggioli, L.: The exact Riemann Solver to the Shallow Water equations for natural channels with bottom steps, *Computers & Fluids*, 254, 105789 (2023). <https://doi.org/10.1016/j.compfluid.2023.105789>.
- [23] Morales de Luna, T., Castro Díaz, M. J., and Parés, C.: Reliability of first order numerical schemes for solving shallow water system over abrupt topography. *Appl. Math. Comput.*, 219, 9012-9032 (2013). <https://doi.org/10.1016/j.amc.2013.03.033>
- [24] Ortega, J.M., Rheinboldt, W.C.: *Iterative Solution of Nonlinear Equations in Several Variables*, New York: Academic Press (1970)
- [25] Osher, S.: Riemann solvers, the entropy condition, and difference approximations. *SIAM J. Numer. Anal.*, 21(2), 217–235 (1984). <https://dx.doi.org/10.1137/0721016>
- [26] Rusanov, V.: The calculation of the interaction of non-stationary shock waves and obstacles. *USSR Computational Mathematics and Mathematical Physics* 1(2), 304-320 (1962). [https://dx.doi.org/10.1016/0041-5553\(62\)90062-9](https://dx.doi.org/10.1016/0041-5553(62)90062-9)
- [27] Sonar, T.: Entropy production in second-order three-point schemes. *Numer. Math.* 62, 371-390 (1992). <https://dx.doi.org/10.1007/BF01396235>
- [28] Stoker, J.J., *Water Waves: The Mathematical Theory with Applications*. John Wiley & Sons, Inc. (1992). <https://doi.org/10.1002/9781118033159>.
- [29] Tadmor, E.: Entropy stability theory for difference approximations of nonlinear conservation laws and related time-dependent problems. *Acta Numerica* 12, 451-512 (2003). <https://dx.doi.org/10.1017/S0962492902000156>
- [30] Zakerzadeh, H., Fjordholm, U.: High-order accurate, fully discrete entropy stable schemes for scalar conservation laws. *IMA J. Numer. Anal.* 36(2), 633–654 (2016). <https://doi.org/10.1093/imanum/drv020>
- [31] Zalesak, S.: Fully multidimensional flux-corrected transport algorithms for fluids. *J. Comput. Phys.* 31(3), 335-362 (1979). [https://dx.doi.org/10.1016/0021-9991\(79\)90051-2](https://dx.doi.org/10.1016/0021-9991(79)90051-2)
- [32] Zalesak, S.T.: The Design of Flux-Corrected Transport (FCT) Algorithms For Structured Grids. In : *Flux-Corrected Transport. Principles, Algorithms, and Applications*, pp. 29-78. Springer, Berlin, Heidelberg (2005). [https://dx.doi.org/10.1007/3-540-27206-2\\_2](https://dx.doi.org/10.1007/3-540-27206-2_2)
- [33] Zhao, N., Wu, H.M.: MUSCL type schemes and discrete entropy conditions. *Journal of Computational Mathematics*, 15(1), 72-80 (1997). <https://www.jstor.org/stable/43692663>